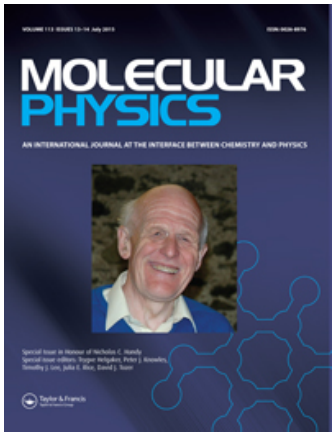

Molecular Physics: An International Journal at the Interface Between Chemistry and Physics
Publication details, including instructions for authors and subscription information:
http://www.tandfonline.com/loi/tmph20

Hybrid variational-perturbation method for calculating ro-vibrational energy levels of polyatomic molecules

A.I. Pavlyuchko[ab], S.N. Yurchenko[b] & Jonathan Tennyson[b]
[a] Department of Physics and Astronomy, Moscow State University of Civil Engineering (MGSU), Moscow, Russia
[b] Department of Physics and Astronomy, University College London, London, UK
Published online: 07 Jan 2015.

Molecular Physics, 2015
Vol. 113, Nos. 13–14, 1559–1575, http://dx.doi.org/10.1080/00268976.2014.992485

INVITED ARTICLE

Hybrid variational–perturbation method for calculating ro-vibrational energy levels of polyatomic molecules

A.I. Pavlyuchko[a,b], S.N. Yurchenko[b] and Jonathan Tennyson[b,*]

[a]*Department of Physics and Astronomy, Moscow State University of Civil Engineering (MGSU), Moscow, Russia;* [b]*Department of Physics and Astronomy, University College London, London, UK*

(*Received 16 July 2014; accepted 20 November 2014*)

A procedure for calculation of rotational–vibrational states of medium-sized molecules is presented. It combines the advantages of variational calculations and perturbation theory. The vibrational problem is solved by diagonalising a Hamiltonian matrix, which is partitioned into two sub-blocks. The first, smaller sub-block includes matrix elements with the largest contribution to the energy levels targeted in the calculations. The second, larger sub-block comprises those basis states which have little effect on these energy levels. Numerical perturbation theory, implemented as a Jacobi rotation, is used to compute the contributions from the matrix elements of the second sub-block. Only the first sub-block needs to be stored in memory and diagonalised. Calculations of the vibrational–rotational energy levels also employ a partitioning of the Hamiltonian matrix into sub-blocks, each of which corresponds either to a single vibrational state or a set of resonating vibrational states, with all associated rotational levels. Physically, this partitioning is efficient when the Coriolis coupling between different vibrational states is small. Numerical perturbation theory is used to include the cross-contributions from different vibrational states. Separate individual sub-blocks are then diagonalised, replacing the diagonalisation of a large Hamiltonian matrix with a number of small matrix diagonalisations. Numerical examples show that the proposed hybrid variational–perturbation method greatly speeds up the variational procedure without significant loss of precision for both vibrational–rotational energy levels and transition intensities. The hybrid scheme can be used for accurate nuclear motion calculations on molecules with up to 15 atoms on currently available computers.

Keywords: molecular rotation; vibration; variational–perturbation theory; infrared spectra; nuclear motion

1. Introduction

Approaches used to compute vibrational–rotational energy levels and wave functions include methods based on perturbation theory, effective Hamiltonians, and the use of the variational principle. Each of these methods has its advantages and disadvantages when used for larger molecules such as those with more than 10 atoms.

Historically, perturbation theory was the first method employed to treat the many-body anharmonic problem [1–9]; see also the review by Klein [10]. Second-order perturbation theory is the most common analytic treatment for estimating the vibrational energy levels and including contributions from terms in the Hamiltonian beyond the harmonic approximation (see, for example, [4,11–13]), as well as infrared (IR) intensities [14]. However, there are drawbacks inherent in this method which prevent the extensive use of it in practice. In particular, the results obtained depend on the specific form of the Hamiltonian and the distribution of degenerate oscillators. Polyatomic molecules often show quasi-degeneracies between vibrational energy levels and the use of second-order perturbation theory can result in significant errors. Furthermore, in practice, anharmonic effects in polyatomic molecules are sufficiently large that they are often not converged with a second-order treatment. As a result, perturbation theory calculations usually overestimate the anharmonic corrections, sometimes by a factor of two; see the final columns of Tables 3 and 4.

Variational methods for the calculation of anharmonic energy levels were developed independently by a number of authors [15–33]. Early implementations in general computer codes focused on the use of basis functions for triatomic molecules [34–37]. More recent developments have involved the increasing use of the discrete variable representation [38–40] and the extension of the work to polyatomic molecules [41–57]. The main advantage of this method is that it allows the almost exact calculations of the vibrational–rotational energy levels and wave functions for a given anharmonic potential [58]. However, variational methods work much better for few-atom systems since the size of the basis set grows factorially with the number of vibrational degrees of freedom in the molecule. Hence, the size of the Hamiltonian matrices, which must be computed and diagonalised, also grows very rapidly. For this reason, variational calculations for polyatomic molecules are

* Corresponding author. Email: j.tennyson@ucl.ac.uk

difficult even on modern computers and, therefore, are not routinely used for molecules with more than six atoms, when only small basis sets can be afforded. The computational errors associated with incomplete basis sets are normally significantly larger than the errors from perturbation approaches; this point will be discussed further in the following section.

The treatment of ro-vibrational states adds extra complexity to the calculation. In this case, a rotational basis set, usually described with analytical rigid-rotor functions, must be introduced. For high rotational quantum number, J, this leads to large Hamiltonian matrices even for small polyatomic molecules. However, a two-step variational procedure can be used to mitigate the effects of this problem [59] meaning that it has long been possible to compute rotational excitation up to dissociation for small molecules [60,61].

There are a number of modifications of the variational method which facilitates (ro-)vibrational calculations on larger molecules: for example, the use of vibrational self-consistent field theory by Gerber and others [62–64]. Bowman and others [65,66] used vibrational configuration interaction (VCI) to reduce the size of the diagonalisation for large molecules. If the molecule has separable degrees of freedom, a significant reduction in the time taken to diagonalise the Hamiltonian matrices can be obtained. Scribano and others [67,68] used a hybrid approach where a modification of the VCI method takes into account the interactions of individual configurations using perturbation theory. Similarly, the general code MULTIMODE [69] allows such treatments of larger systems [70] with approximations involving the degree of coupling between vibrational modes.

Here we propose a new hybrid variational–perturbation theory method based on a physically reasonable division of the large, full, variational Hamiltonian matrix into weakly interacting sub-blocks. Second-order perturbation theory is used to include cross-interaction effects between these sub-blocks, which are then diagonalised separately. This allows one to replace a single diagonalisation of a large Hamiltonian matrix by a series of diagonalisations of much smaller sub-matrices. We show that our hybrid method can greatly accelerate the variational procedure by eliminating diagonalisation of large matrices without significant loss of precision in the computed vibrational–rotational energy levels and the intensity of transitions between them. This hybrid scheme is able to perform calculations for large molecules containing up to 15 atoms on currently available computers. Finally, we note that a different version of the hybrid variational–perturbation approach has recently been proposed by Fabri *et al.* [71] and implemented in the general Eckart–Watson Hamiltonian code DEWE [72]. Their hybrid scheme uses a traditional single-state ro-vibrational–perturbation method based on the variationally computed vibrational ($J = 0$) eigenfunctions as a zero-order solution, where the vibrational problem is solved variationally and ro-vibrational energies are derived using the second-order perturbation theory expressions. This is different from our two-step hybrid scheme, where the perturbation method is an integral part of calculations. We believe that this is the key to extending variational calculations to larger molecules.

The method we propose is not dependent on the precise form of the Hamiltonian. Instead, the requirement of the Hamiltonian is that it should result in a diagonally dominant matrix representation. For semi-rigid molecules, this criterion has naturally satisfied the Eckart–Watson Hamiltonian [73] as well as number of related Hamiltonians [74–76]. However, the method is unlikely to perform so well for Hamiltonians whose emphasis is not on making producing diagonally dominant matrices such as those expressed in polyspherical coordinates [77]. In this work, all calculations are performed using ANGMOL [74], a variational program for calculating ro-vibrational spectra of general polyatomic molecules. ANGMOL uses a Hamiltonian expressed in curvilinear internal coordinates and an Eckart embedding that is discussed briefly in the appendix and extensively elsewhere [74].

2. A variational method for vibrational energy levels

To start, we consider the nature of the error arising from the use of the variational method for calculating vibrational ($J = 0$) energy levels of polyatomic molecules. In the variational Rayleigh–Ritz procedure, the wave function, ψ_n, is generally approximated by a finite expansion,

$$\psi_n = \sum_i C_i^{(n)} \varphi_i, \tag{1}$$

in terms of some appropriate basis functions φ_i. Mathematically, this procedure is equivalent to finding the eigenvalues and eigenvectors of the Hamiltonian matrix whose elements are given by

$$H_{ij} = \langle \varphi_i | \hat{H}_v | \varphi_j \rangle. \tag{2}$$

Eigenvalues of this matrix give values of the vibrational energy levels, E_n, and the eigenvectors, $C_i^{(n)}$, give the wave function, ψ_n, when combined with the basis functions. For ease of use and better convergence of the basis functions, the φ_i are generally chosen to form a complete orthonormal set. The exact values of the energy levels and eigenfunctions are only guaranteed with an infinite number of basis functions.

The accuracy of the calculated energies depends on the number of basis functions used. As the basis set is extended, the calculated energy levels tend (mostly smoothly and monotonically) to their theoretical limit. The variational limit for a group of (lowest) energy levels is reached when the number of basis functions is sufficient for the chosen energy levels to differ from the exact value by less

than some prescribed error. The physical meaning of the variational limit is that basis functions representing highly excited vibrational levels make only a small contribution to the eigenfunctions of the low-lying levels.

The number of basis functions needed to reach the variational limit depends on the number of energy levels to be calculated. In general, the greater the number of energy levels calculated, the larger the number of basis functions required. However, a good choice of basis functions also speeds the convergence: the closer the basis functions are to desired eigenfunctions, the fewer of them are required to achieve the variational limit. Mathematically, this means that the off-diagonal matrix elements (H_{ij}) become small, the eigenvalues become close to the corresponding diagonal element (H_{ii}), and the corresponding eigenvectors tend towards being unit vectors.

Details of our method are give in Appendix. We start by defining the vibrational basis as a product of one-mode functions,

$$\varphi_i = \prod_{m=1}^{N_c} \phi_m(v_m), \tag{3}$$

where $\phi_m(v_m)$ is either a Morse or a harmonic oscillator function, v_m is the excitation number of the mth oscillator, and N_c is the number of vibrational degrees of freedom. Morse oscillator functions are commonly used for the X–H stretches and other stretching motion whose vibrations are strongly anharmonic, such as doubly-bonded CO. Harmonic oscillator functions are used for skeletal bonds in molecules with small anharmonicity, for example, the CC bonds in hydrocarbons, and for all deformation (angular) oscillations. This form of the basis set helps to reduce the off-diagonal elements in the Hamiltonian matrix and thus has been found to give rapid convergence to the variational limit.

In variational procedures it is often considered desirable to use a complete, orthonormal basis. The bound states of the Morse oscillator form a variational basis of finite length basis and so are, strictly speaking, not longer complete. It is possible to develop a complete set based on the Morse oscillators [28]; however, our practical computation shows that rapid convergence can be achieved with a finite number of Morse oscillators allowing the variational limit to be reached.

Our implementation relies on the particular structure of the Hamiltonian matrix ordered by increasing polyad (total vibrational excitation) number, N_V:

$$N_V = \sum_{m=1}^{N_c} a_m v_m, \tag{4}$$

where a_m is some integer weighting which is often roughly proportional to the inverse of the frequency [76]. For simplicity in this work, we use $a_m = 1$ for all m. This gives the size of the basis set, $M_B^{\max}$, in terms of the maximum polyad number, $N_V^{\max}$:

$$M_B^{\max} = \frac{(N_V^{\max} + N_c)!}{N_V^{\max}! N_c!} = \prod_{i=1}^{N_c} \left(N_V^{\max} + i\right)/i, \tag{5}$$

which increases factorially with the number of vibrational degrees of freedom, N_c.

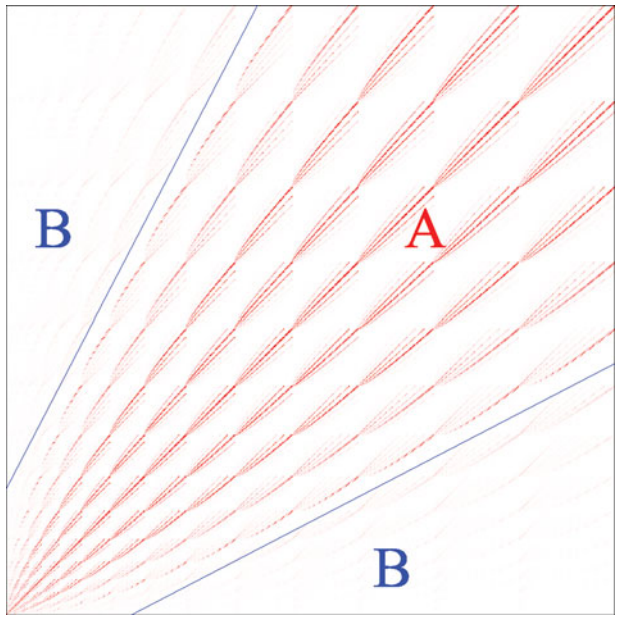

Figure 1. Semi-banded structure of the vibrational ($J = 0$) Hamiltonian matrix for water ($N_V^{\max} = 16$, $M_B^{\max} = 969$): Region A contains large (near-)diagonal elements; Region B contains only small off-diagonal elements. The blue continuous lines are used to separate the two regions. The brightness of the red points is proportional to the magnitude of the individual matrix elements.

With this definition of the basis set, the Hamiltonian matrix has a semi-banded structure, as shown in Figure 1, and can be factorised into two regions: the region around the diagonal (Region A), containing large off-diagonal elements, and the outer region (Region B) with 'small' or zero off-diagonal elements. The width of the band, as discussed in Appendix, depends on the form of the Hamiltonian and obviously on the precise definition of 'small'. For example, with a potential function represented as a fourth-order polynomial in terms of the coordinate displacements and harmonic oscillator basis functions, the band only includes matrix elements with excitations whose basis functions $\phi_m(v_m)$ are separated from the diagonal by $\Delta v_m \leq 4$. The use of the Morse oscillator basis functions gives a similar picture. Clearly distinguishable in Figure 1 are eight off-diagonal bands corresponding to elements connected by $\Delta v_m = \pm 1$, ± 2, ± 3, and ± 4. Thus, for a fourth-order, anharmonic potential function, all matrix elements separated by $\Delta v_m > 4$ lie in Region B which becomes increasingly large as either

N_V or N_c increases. This rule has similarities with the well-known Slater's rules for configuration interaction matrix elements in electronic structure calculations.

As an example, we use the program ANGMOL to compute the vibrational band origins and corresponding band intensities for H_2O and HNO_3. In these calculations, we employ semi-empirical potential energy functions represented as fourth-order polynomials which were obtained by fitting the corresponding potential parameters to experimentally derived energies [78,79]. These empirical potential energy functions reproduce the experimental vibrational term values of the fundamental and the first overtone states of HNO_3 and H_2O with the root-mean-square (rms) errors less than 0.1 and 0.4 cm^{-1}, respectively. Initial values of the potential parameters were obtained using *ab initio* calculations at the CCSD(T)/aug-cc-pVQZ level of theory. The corresponding dipole moments were represented in the form of a second-order polynomial fitted to the CCSD(T)/aug-cc-pVQZ *ab initio* values. Full details will be given elsewhere [80].

All calculations were performed using curvilinear vibrational coordinates (see Appendix). To represent the stretching coordinates, we use Morse coordinates $q_i = 1-\exp(\alpha_i \Delta r_i)$, where Δr_i in the bond length displacements of the ith bond and α_i is the standard Morse parameter. Valence angles were represented by $q_j = \cos\theta_j - \cos\theta_e$, where θ_j and θ_e are the jth inter-bond angle and its equilibrium value, respectively. Basis functions were constructed as a direct product of the Morse oscillator functions for the stretches and harmonic oscillator functions for the angles. The harmonic part of the Hamiltonian is constructed to be diagonal for the bending part.

This form of variational basis functions has the advantage that the vibrational Hamiltonian matrix has relatively small off-diagonal elements, i.e. it is close to a diagonal form. This is due to (1) the property of the Morse oscillators which give a good description of the stretching modes and (2) small bending anharmonic terms. Besides, in this basis, the Hamiltonian matrix elements all have simple analytical forms and thus can be efficiently evaluated.

Tables 1 and 2 present the calculated values of the wavenumbers and intensities of the vibrational transitions for H_2O and HNO_3 as a function of the number of basis functions used in the variational calculations. In the following, the parameter N_V^{target} ($N_V^{target} \le N_V^{max}$) will be used to reference the polyad number for energy values targeted in the variational calculations and M_V^{target} ($M_V^{target} \le M_V^{max}$) to reference the corresponding number of vibrational states. The results for the water molecule suggest that to compute

Table 1. Fully variational calculation of the vibrational band origins (upper row, cm^{-1}) and vibrational band intensities (lower row, km $mole^{-1}$) for H_2O as a function of total vibrational excitation number, N_V^{max}, and number of basis functions, M_B^{max}.

	N_V^{max}/M_B^{max}											
Transition	20/1771	11/364	10/286	9/220	8/165	7/120	6/84	5/56	4/35	3/20	2/10	1/4
0 1 0	1595.0	1595.0	1595.0	1595.0	1595.0	1595.1	1595.2	1595.3	1598.4	1601.6	1626.1	1623.4
	68.72	68.72	68.72	68.72	68.73	68.73	68.73	68.75	68.85	68.80	70.11	69.78
0 2 0	3152.0	3152.0	3152.1	3152.2	3152.5	3153.3	3153.5	3163.0	3173.4	3211.5	3236.0	
	0.424	0.425	0.425	0.425	0.426	0.428	0.432	0.443	0.502	0.636	0.773	
1 0 0	3656.8	3656.8	3656.8	3656.8	3656.8	3656.9	3656.9	3657.1	3657.9	3659.3	3682.0	3672.4
	2.807	2.807	2.806	2.806	2.806	2.805	2.804	2.796	2.773	2.691	2.638	1.316
0 0 1	3755.5	3755.5	3755.5	3755.5	3755.5	3755.5	3755.5	3755.6	3756.0	3756.4	3768.3	3767.4
	49.55	49.55	49.55	49.55	49.55	49.55	49.55	49.56	49.54	49.53	49.70	52.41
0 3 0	4666.8	4667.1	4667.6	4668.9	4671.2	4671.7	4694.7	4716.8	4766.5	4820.7		
	0.080	0.080	0.080	0.080	0.079	0.078	0.078	0.071	0.066	0.002		
1 1 0	5234.6	5234.6	5234.6	5234.7	5234.8	5235.2	5235.7	5239.7	5247.4	5297.2	5306.8	
	0.083	0.083	0.083	0.083	0.083	0.083	0.084	0.084	0.090	0.076	0.024	
0 1 1	5331.2	5331.2	5331.2	5331.2	5331.3	5331.4	5331.6	5333.8	5337.2	5365.8	5383.7	
	3.840	3.840	3.840	3.840	3.840	3.840	3.841	3.837	3.856	3.853	3.571	
1 2 0	6773.7	6773.9	6774.2	6774.8	6776.2	6777.6	6789.2	6808.7	6883.0	6914.0		
	0.016	0.016	0.016	0.016	0.017	0.017	0.018	0.021	0.037	0.021		
0 2 1	6870.6	6870.6	6870.7	6870.9	6871.6	6872.0	6878.8	6887.2	6935.1	6962.3		
	0.044	0.044	0.044	0.044	0.044	0.044	0.045	0.049	0.078	0.056		
2 0 0	7202.0	7202.0	7202.0	7202.0	7202.1	7202.3	7202.6	7203.8	7207.9	7241.0	7244.8	
	0.387	0.387	0.387	0.387	0.387	0.387	0.386	0.383	0.368	0.370	0.387	
1 0 1	7250.1	7250.1	7250.1	7250.1	7250.2	7250.3	7250.5	7251.2	7253.8	7279.2	7290.7	
	3.037	3.037	3.037	3.037	3.036	3.036	3.035	3.032	3.007	3.042	3.268	
0 0 2	7444.7	7444.7	7444.7	7444.7	7444.7	7444.8	7444.9	7445.4	7447.0	7462.7	7488.5	
	0.027	0.027	0.027	0.027	0.027	0.027	0.027	0.027	0.027	0.032	0.037	
3 0 0	10,599.3	10,599.4	10,599.4	10,599.5	10,599.8	10,600.4	10,601.9	10,611.9	10,649.9	10,661.9		
	0.023	0.023	0.023	0.023	0.023	0.023	0.023	0.021	0.020	0.031		
0 0 3	11,032.7	11,032.7	11,032.8	11,032.8	11,032.9	11,033.1	11,033.5	11,036.1	11,054.7	11,106.8		
	0.004	0.004	0.004	0.004	0.004	0.004	0.004	0.004	0.003	0.007		

Table 2. Fully variational calculation of the vibrational band origins (upper row, cm^{-1}) and vibrational band intensities (lower row, km $mole^{-1}$) for HNO_3 as a function of total vibrational excitation number, N_V^{max}, and number of basis functions, M_B^{max}.

	N_V^{max}/M_B^{max}								
Transition	9/48620	8/24310	7/11440	6/5005	5/2002	4/715	3/220	2/55	1/10
ν_9	458.8	459.5	460.4	466.3	465.2	509.3	476.1	945.6	485.5
	107.3	107.5	107.7	109.0	108.9	117.8	112.0	13.1	114.5
ν_8	581.2	582.9	583.1	592.5	590.7	651.7	616.0	1041.3	688.4
	7.52	7.54	7.63	7.77	7.93	8.94	8.9	11.7	14.2
ν_7	648.5	649.8	652.1	662.6	663.5	731.0	695.3	1315.3	781.8
	10.5	10.6	10.4	10.8	10.3	11.1	9.58	171.0	6.26
ν_6	763.5	764.0	764.4	769.9	767.0	810.3	772.2	750.6	780.2
	7.90	7.90	7.90	7.95	7.91	8.27	7.99	158.6	8.05
ν_5	881.3	883.1	885.8	896.3	899.0	964.1	934.6	1351.3	1047.1
	106.7	110.3	126.1	118.8	148.6	94.4	140.6	171.3	105
$2\nu_9$	899.5	901.4	907.8	915.8	955.6	982.7	1199.7		
	52.3	48.6	32.9	40.9	8.02	70.0	1.44		
$\nu_6 + \nu_9$	1207.8	1209.1	1215.1	1219.7	1253.2	1272.2	1519.9		
	9.69	9.74	10.5	10.0	18.8	9.62	5.29		
$3\nu_9$	1301.2	1310.0	1323.4	1391.8	1406.5	1671.5	1409.8		
	0.266	0.272	0.263	0.043	0.181	0.115	0.007		
ν_4	1306.8	1297.4	1302.6	1311.3	1316.6	1368.1	1321.8	1629.2	1359.3
	55.6	46.5	74.2	68.1	78.1	40.3	52.2	37.3	42.5
ν_3	1327.5	1328.9	1331.6	1343.6	1347.8	1407.4	1369.8	1744.0	1484.0
	223.7	227.0	209.6	163.5	122.5	256.7	242.2	173.3	191.9
$4\nu_9$	1702.5	1723.0	1768.0	1836.2	2085.6	2178.9			
	13.8	3.37	0.185	0.009	0.030	0.074			
ν_2	1710.6	1711.6	1712.7	1723.4	1722.2	1791.8	1755.0	2141.7	1875.0
	348.0	359.3	363.1	365.3	358.8	373.4	340.2	390.7	283.2
ν_1	3552.0	3552.4	3553.3	3558.3	3555.8	3599.0	3559.8	3843.1	3565.5
	35.3	84.4	39.8	82.1	83.7	79.9	67.6	86.8	90.9

all vibrational levels associated with the polyad number $N_V \leq N_V^{target}$ to better than 5 cm^{-1}, the basis set must include functions with N_V^{max} at least up to $N_V^{target} + 4$. For example, to obtain all energies up to the second overtones ($N_V^{target} = 3$) with this accuracy, N_V^{max} must be at least 7. This is in accord with our assumption that for the potential energy function given as a fourth-order polynomial, the large matrix elements which belong in Region 1 are all associated with functions given by $N_V \leq N_V^{target} + 4$.

Calculating all $N_V \leq N_V^{target}$ vibrational term values to an accuracy better than 0.3 cm^{-1} requires basis functions with $N_V^{max} \geq N_V^{target} + 8$. This means that the Hamiltonian matrix must include all the basis functions for which the difference in v_m is up to 8.

For water, using the lowest possible basis, i.e. $N_V^{max} = N_V^{target}$, gives errors of 28 cm^{-1} for the ν_2 fundamental band, 84 cm^{-1} for the first overtone $2\nu_2$, and 154 cm^{-1} for $3\nu_2$ (see Table 1). For HNO_3, the situation is even worse, with $N_V^{max} = N_V^{target} + 1$, the band centres of the fundamentals are not reproduced to within 500 cm^{-1}.

It is important to note that the number of the target energy levels defined by N_V^{target} grows rapidly with the number of degrees of freedom N_c. For a triatomic molecule like water ($N_c = 3$), to reach an accuracy better than 0.5 cm^{-1} for the fundamental bands only ($N_V^{target} = 1$, $N_V^{max} = 9$) requires $M_B^{max} = 220$ basis functions. For a pentatomic molecule, such as HNO_3 ($N_c = 9$), this requires $M_B^{max} = 48{,}620$ basis functions and for an eight-atom molecule such as C_2H_6 ($N_c = 18$), M_B^{max} is 4,686,825.

The vibrational energies of polyatomic molecules are often characterised by (accidental) resonances, such as Fermi resonances, resulting from strong mixing between vibrationally excited states. One consequence of this is that for HNO_3 N_V^{max} is increased to $N_V^{max} \geq N_V^{target} + 9$. Comparison of columns 2 of Tables 2 and 4 shows that even when for $M_B^{max} = 48{,}620$ basis functions corresponding to $N_V^{max} = 9$, the convergence of the fundamental energy levels, i.e. $N_V^{target} = 1$, is only good to 4 cm^{-1}.

For nitric acid, the resonances can also give rise to large errors in band intensities for vibrational states involved in these resonances, especially when small basis sets are used. However, the sum of the band intensities for all resonant states is less sensitive to the size of the basis set. We note, however, that for water, even individual vibrational band intensities show relatively small dependence on the basis set size (see Table 1).

Tables 1 and 2 also show that the stretching energy levels converge faster, requiring less basis functions, than the bending modes. This is because the Morse oscillators are more compact than the harmonic oscillator basis functions

and also because the stretching quanta of hydrogen bonds are normally about two times larger than that of the bending modes, i.e, they take fewer stretching quanta to reach the same energy. However, the harmonic oscillator functions used for the bending modes also represent a reasonable choice giving small coupling matrix elements, which satisfy the requirements of perturbation theory.

3. A hybrid method for calculating vibrational energy levels

Variational calculations on many-atom systems rapidly become impractical. To address this problem, we implement a mixed variational–perturbation theory approach. The idea is based on the observation that the calculated energies and wave functions of the lower lying vibrational levels depend differently on different parts of the Hamiltonian matrix. As described above, the general Hamiltonian matrix can be factorised into two regions as illustrated in Figure 2. The first region contains the zeroth-order contribution to the calculated vibrational energies as well as all other states strongly coupled to them. As noted above, these strongly coupled levels are those for which the Hamiltonian matrix contains large off-diagonal elements with the states of interest. For a potential function represented as a fourth-order polynomial, the first block should contain couplings to the targeted states with all contributions with $\Delta v_m \leq 4$.

The second region of the matrix is generally much larger. This region includes all the remaining basis states that only have a small effect on the calculated energy levels in question. These basis states are the ones for which the polyad numbers N_V differ by more than 4 from those of the levels of interest, $N_V > N_V^{\text{target}} + 4$, because the corresponding off-diagonal elements are small.

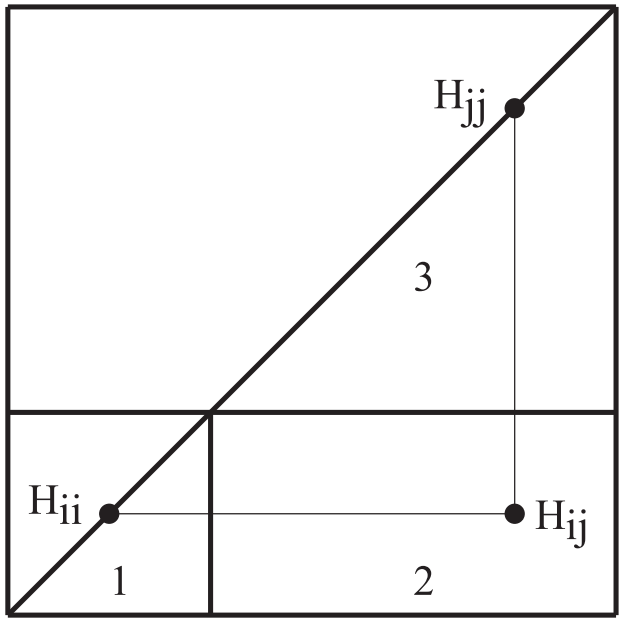

Figure 2. Block structure of the vibrational Hamiltonian matrix. Region 1: matrix elements with the largest contributions to the target energy levels ($N_V \leq N_v^{\text{target}} + 4$); Region 2 contains elements with small contributions to these states. The contribution from elements in Region 3 is disregarded.

The essence of our method is that instead of diagonalising the whole Hamiltonian matrix, we diagonalise the smaller block 1 (see Figure 2) with the matrix elements corrected by the second-order perturbative contributions from Region 2 as described in detail below.

Assuming the size $M_B^{\max}$ of the overall Hamiltonian matrix is defined by $N_V^{\max}$ in connection with Equation (5) and the size of block 1, $M_B^{(1)}$, is given by

$$M_B^{(1)} = \frac{(N_V^{(1)} + N_c)!}{N_V^{(1)}! N_c!} = \prod_{i=1}^{N_c} \left(N_V^{(1)} + i\right)/i, \tag{6}$$

where $N_V^{(1)}$ is the number of the largest polyad included in block 1. To reach an accuracy of 1 cm^{-1} or better, the following two conditions have to be met: $N_V^{\max} \geq N_V^{\text{target}} + 8$ and $N_V^{(1)} \geq N_V^{\text{target}} + 4$.

In the first step of our approach, all the matrix elements from block 1 are computed along with the diagonal matrix elements of block 3. The second step involves computing the off-diagonal elements of block 2 and accounting for their effect on the matrix elements of the block 1 using one Jacobi rotation [81,82]. Considering a contribution from the block 2 off-diagonal element H_{ij}, which couples the diagonal elements H_{ii} in block 1 and H_{jj} in block 3 (see Figure 2), these two diagonal elements are perturbatively adjusted using the Jacobi formula as follows:

$$\tilde{H}_{ii} = H_{ii} - \sum_{j \in \text{block2}} \Delta E_{ij}, \tag{7}$$

where

$$\Delta E_{ij} = \frac{\text{sign}(\sigma_{ij}) H_{ij}}{|\sigma_{ij}| + \sqrt{1 + \sigma_{ij}^2}} \tag{8}$$

and

$$\sigma_{ij} = \frac{(H_{jj} - H_{ii})}{2H_{ij}}. \tag{9}$$

Here H_{ii} is an initial (unperturbed) diagonal element and $\tilde{H}_{ii}$ is an adjusted one. This formula automatically allows for cases where the unperturbed vibrational states are (quasi-) degenerate, i.e. $H_{ii} \approx H_{jj}$. In the absence of the degeneracy, $|H_{ij}| \ll |H_{jj} - H_{ii}|$, we have $\Delta E_{ij} \approx H_{ij}^2/(H_{jj} - H_{ii})$, which is equivalent to the energy correction given by second-order perturbation theory (see e.g. [2]). Similarly, if there is degeneracy or quasi-degeneracy $|H_{ij}| \approx |H_{jj} - H_{ii}|$, we have $\Delta E_{ij} \leq H_{ij}$ and for degeneracy $|H_{ij}| \gg |H_{jj} - H_{ii}|$, we

have $\Delta E_{ij} \approx H_{ij}$. That is, $H_{ij}^2/(H_{jj} - H_{ii}) \leq \Delta E_{ij} \leq H_{ij}$ is always satisfied.

Strictly speaking, an off-diagonal element H_{ij} in block 2 should be included as perturbative contribution both to the relevant diagonal H_{ii} and off-diagonal H_{ik} elements from block 1. However, the changes to the off-diagonal are of the secondorder leading to small contributions and are thus omitted here without significant loss of accuracy, as will be shown later.

In the final step of the algorithm, block 1 of the corrected Hamiltonian matrix is diagonalised. The resulting eigenfunctions are represented as expansions in terms of the basis functions associated with block 1 only, while the eigenvalues include contributions from all three regions of the matrix.

As in the examples above, we use H_2O and HNO_3 to illustrate the method (see also [83], where VPT2 was used to study the IR spectroscopic properties of HNO_3). Tables 3 and 4 show similar results obtained using our hybrid method, where the vibrational term values calculated with the size of block 1, $M_B^{(1)}$, increasing. We note that when $N_V^{(1)} = N_V^{\max}$, our hybrid method automatically becomes a full variational calculation.

The hybrid method provides accurate results for the vibrational energy levels even when the dimension of the final diagonalised block $M_B^{(1)}$ is much smaller than the dimension of the full Hamiltonian matrix $M_B^{\max}$. For example, to calculate the vibrational energy levels of water with an average accuracy of 1 cm^{-1}, it is sufficient to explicitly include the basis functions with $N_V^{(1)} \geq N_V^{\text{target}} + 4$. That is, block 1 includes all the larger off-diagonal elements (at least $N_V^{\text{target}} + 4$) and block 2 contains the smaller off-diagonal elements contributing to the target vibrational energies (at least $N_V^{\text{target}} + 8$).

This reduction is especially valuable for larger molecules. For example, the $N_V^{(1)} = N_V^{\text{target}} + 4$ rule for the eight-atomic molecule C_2H_6 ($N_c = 18$) means that to calculate the fundamental band centres to within 1 cm^{-1}, the dimension of block 1 is only $M_B^{(1)} = 33{,}649$ ($N_V^{(1)} = 5$), while the full size of the Hamiltonian matrix is $M_B^{\max} = 4{,}686{,}825$ ($N_V^{\max} = 9$). For HNO_3, we have $M_B^{(1)} = 2002$ and $M_B^{\max} = 48{,}620$ ($N_V^{\max} = 9$).

However, in case of a strong Fermi resonance between vibrational states, the accuracy condition must be increased at least by 1 unit. For example, in order to obtain all vibrational term values of HNO_3 defined by the polyad number

Table 3. Calculated values of the vibrational band origins (upper row, cm^{-1}) and vibrational band intensities (lower row, km $mole^{-1}$) for H_2O using our hybrid method and perturbation theory (PT).

	$N_V^{\max}$=20 , $M_B^{\max}$=1771 , $N_V^{(1)}/M_B^{(1)}$												
Transition	20/1771	11/364	10/286	9/220	8/165	7/120	6/84	5/56	4/35	3/20	2/10	1/4	PT
0 1 0	1595.0	1595.0	1595.0	1595.0	1594.9	1595.0	1595.0	1594.8	1594.8	1594.6	1594.7	1593.8	1593.7
	68.72	68.72	68.72	68.72	68.72	68.72	68.72	68.73	68.69	68.47	68.72	68.49	68.58
0 2 0	3152.0	3152.0	3152.0	3151.9	3151.9	3152.1	3151.2	3152.1	3152.8	3147.8	3146.5		3146.6
	0.424	0.424	0.424	0.424	0.424	0.425	0.426	0.429	0.484	0.594	0.705		0.442
1 0 0	3656.8	3656.8	3656.8	3656.8	3656.8	3656.8	3656.8	3656.8	3656.8	3657.0	3664.5	3660.2	3660.1
	2.807	2.807	2.807	2.807	2.807	2.807	2.806	2.803	2.787	2.740	2.700	1.324	2.653
0 0 1	3755.5	3755.5	3755.5	3755.5	3755.5	3755.5	3755.4	3755.4	3755.1	3754.5	3751.1	3755.3	3756.6
	49.55	49.55	49.55	49.55	49.55	49.55	49.55	49.55	49.52	49.45	49.42	52.24	49.83
0 3 0	4666.8	4666.6	4666.1	4666.5	4667.1	4663.6	4668.1	4672.2	4654.0	4651.7			4656.0
	0.080	0.080	0.080	0.080	0.080	0.079	0.080	0.075	0.072	0.002			0.073
1 1 0	5234.6	5234.6	5234.6	5234.6	5234.6	5234.7	5234.6	5234.6	5235.9	5250.4	5248.5		5242.7
	0.083	0.083	0.083	0.083	0.083	0.083	0.083	0.084	0.088	0.082	0.026		0.115
0 1 1	5331.2	5331.2	5331.2	5331.1	5331.1	5331.1	5331.0	5329.7	5327.8	5320.6	5325.6		5331.9
	3.840	3.840	3.840	3.840	3.840	3.840	3.840	3.838	3.861	3.885	3.568		3.686
1 2 0	6773.7	6773.6	6773.6	6773.7	6774.1	6773.3	6774.1	6778.9	6794.0	6802.8			6786.5
	0.016	0.016	0.016	0.016	0.016	0.016	0.017	0.018	0.024	0.012			0.026
0 2 1	6870.6	6870.6	6870.4	6870.4	6870.4	6869.8	6866.8	6863.8	6850.7	6850.6			6866.3
	0.044	0.044	0.044	0.043	0.044	0.044	0.043	0.046	0.062	0.040			0.094
2 0 0	7202.0	7202.0	7202.0	7202.0	7202.0	7202.0	7202.0	7201.8	7202.5	7214.9	7206.2		7202.5
	0.387	0.387	0.387	0.387	0.387	0.387	0.387	0.385	0.377	0.375	0.386		0.369
1 0 1	7250.1	7250.1	7250.1	7250.0	7250.0	7250.0	7250.0	7249.4	7249.0	7253.2	7252.4		7255.5
	3.037	3.037	3.037	3.037	3.037	3.037	3.037	3.035	3.021	3.056	3.259		3.008
0 0 2	7444.7	7444.7	7444.7	7444.7	7444.6	7444.6	7444.6	7444.0	7443.0	7438.5	7449.4		7452.2
	0.027	0.027	0.027	0.027	0.027	0.027	0.027	0.027	0.027	0.033	0.036		0.023
3 0 0	10,599.3	10,599.3	10,599.2	10,599.2	10,599.2	10,599.1	10,598.4	10,599.8	10,613.4	10,603.1			10,604.9
	0.023	0.023	0.023	0.023	0.023	0.023	0.023	0.023	0.023	0.031			0.026
0 0 3	11,032.7	11,032.7	11,032.7	11,032.7	11,032.6	11,032.5	11,031.5	11,029.8	11,022.3	11,046.0			11,041.2
	0.004	0.004	0.004	0.004	0.004	0.004	0.004	0.004	0.003	0.007			0.006

Table 4. Calculated values of vibrational band origins (upper row, cm^{-1}) and vibrational band intensities (lower row, km $mole^{-1}$) for HNO_3 using our hybrid method and perturbation theory (PT).

	N_V^{max}=14 , M_B^{max}=817190 , $N_V^{(1)}/M_B^{(1)}$									
Transition	9/48,620	8/24,310	7/11,440	6/5005	5/2002	4/715	3/220	2/55	1/10	PT
ν_9	458.2	457.4	457.7	453.6	455.0	448.3	442.0	486.7	458.5	458.7
	107.2	107.0	107.0	105.9	106.2	102.9	103.6	96.3	108.0	107.5
ν_8	580.3	578.8	578.3	571.8	571.8	559.6	554.1	601.5	574.2	583.4
	7.47	7.39	7.40	6.99	6.96	6.40	6.08	6.88	11.4	19.8
ν_7	646.7	644.2	644.7	633.8	635.3	620.4	610.0	672.9	635.5	652.5
	10.5	10.5	10.5	10.7	10.4	10.9	10.8	9.18	8.82	9.05
ν_6	763.2	762.4	762.9	759.0	760.7	753.7	750.6	791.3	762.2	761.2
	7.90	7.89	7.88	7.83	7.81	7.64	7.72	6.83	7.84	8.02
ν_5	879.1	877.8	876.4	870.6	868.6	856.5	857.0	918.7	904.5	899.5
	96.2	100.4	86.2	99.0	86.9	45.9	133.9	33.7	85.7	4.42
$2\nu_9$	896.4	895.3	893.6	887.3	887.0	874.5	911.5	948.8		954.1
	62.7	58.3	73.4	58.5	71.4	107.5	8.20	95.7		204.8
$\nu_6 + \nu_9$	1205.4	1204.8	1200.8	1198.9	1195.4	1179.3	1212.5	1226.6		1212.6
	9.53	9.60	7.45	6.20	8.17	6.88	5.55	10.4		2.80
$3\nu_9$	1288.8	1285.0	1280.7	1274.7	1274.1	1278.2	1318.7			1323.2
	0.262	0.250	0.259	0.273	0.234	0.130	0.016			0.032
ν_4	1302.9	1301.6	1300.3	1293.1	1294.1	1277.5	1275.2	1300.8	1255.1	1224.0
	81.0	82.6	88.2	94.1	89.0	76.5	75.2	32.6	38.0	46.2
ν_3	1326.2	1324.9	1324.7	1318.9	1319.4	1311.7	1306.1	1385.0	1355.4	1409.6
	220.2	217.8	216.5	210.5	210.6	221.7	114.6	218.1	185.5	53.2
$4\nu_9$	1662.8	1660.4	1656.8	1656.0	1669.4	1691.0				1728.0
	0.727	0.721	0.641	0.489	0.787	67.9				0.655
ν_2	1709.5	1708.1	1708.1	1702.7	1701.7	1694.2	1692.5	1770.8	1745.2	1666.0
	360.3	318.0	358.3	350.0	250.2	174.0	332.6	288.2	252.3	272.8
ν_1	3551.6	3550.7	3551.4	3546.8	3550.2	3542.0	3542.3	3592.9	3555.5	3553.1
	83.1	68.3	83.1	72.6	79.9	81.6	85.6	59.6	89.9	84.8

$N_V \leq N_V^{target}$ to within 4.0 cm^{-1}, the basis set should include contributions from at least $N_V^{(1)} \geq N_V^{target} + 5$ (see Table 4).

Even with very small basis sets, the hybrid method gives reasonable results. For example, with the minimum possible size defined by $N_V^{(1)} = N_V^{target}$, the error in the band centres of ν_2, $2\nu_2$, and $3\nu_2$ of H_2O is 2, 6, and 15 cm^{-1}, respectively, which can be compared to the error of 28, 84, and 154 cm^{-1}, respectively, obtained using the purely variational procedure with the same basis set size. This and other examples collected in Tables 3 and 4 show that our hybrid method inherits the advantage of perturbation theory which performs reasonably well with small basis sets.

In the limit of $M_B^{(1)} = 0$, our variational–perturbation method turns into the pure perturbation calculation with the perturbation treated numerically rather than analytically. For comparison, Tables 3 and 4 also give results obtained from perturbation theory using a single Jacobi rotation for each off-diagonal element.

Tables 3 and 4 also illustrate the performance of the hybrid approach for the vibrational band intensities of these two molecules. These results suggest that for small basis sets, the hybrid intensities are slightly better than intensities obtained using a direct variational treatment of the same size. This is due to the reasonable quality achieved, even with small basis sets, of the corresponding energy levels and eigenfunctions.

It should be noted that the hybrid method requires that the off-diagonal elements H_{ij} of block 2 are small compared to the elements of block 1. This requirement can be satisfied if basis functions are close to the true eigenfunctions. Our tests show that the Morse oscillators used for the stretching coordinates and harmonic oscillators used for the other degrees of freedom satisfy this criterion.

Finally, we note that it is not necessary to compute off-diagonal elements in block 3. This means that the total number of the off-diagonal elements calculated is $M_B^{(1)} \times M_B^{max}$, which is much less than the overall size of the Hamiltonian matrix $M_B^{max} \times M_B^{max}$.

4. Hybrid method for calculating ro-vibrational energy levels

Inclusion of rotational motion into the problem adds an extra level of complexity, especially when highly excited rotational states are required. The dimension of the ro-vibrational problem $M_B^{(rv)}$ is normally increased by the factor of $(2J + 1)$, where J is the total angular momentum quantum number. In the variational approach, this leads to

matrices which can be several order of magnitude larger than the corresponding pure vibrational ($J = 0$) Hamiltonian matrices.

In order to make the vibrational part of the basis set more compact, we construct the ro-vibrational basis set as a direct product of the rigid-rotor wave functions $|J, k, m\rangle$ and a set of selected vibrational eigenfunctions of the $J = 0$ problem obtained as described above. This approach is sometimes referenced in the literature as the $J = 0$ contraction [84]. Let us use $M_B^{\text{vib}} \geq M_B^{\text{target}}$ as the number of vibrational eigenstates for this purpose. M_B^{vib} can be significantly reduced compared to the total number of vibrational states, $M_B^{(1)}$, from the previous step as defined by the size of block 1. This is because not all of the $M_B^{(1)}$ vibrational states are equally important for the target vibrational bands M_B^{target}. Indeed, because our expansion of the kinetic energy operator is truncated at the second order (see Appendix), many matrix elements with $\Delta v > 2$ are either exactly zero (for the harmonic oscillators) or very small.

As an example, consider the situation where we would like to compute a spectrum involving all ro-vibrational energies of HNO_3 up to $hc \cdot 4500\ \text{cm}^{-1}$. This range corresponds to $N_V^{\text{target}} = 4$ or $M_B^{\text{target}} = 715$. From our experience of the HNO_3 molecule, the corresponding ro-vibrational basis set has to include excitations at least up to $hc \cdot 6500\ \text{cm}^{-1}$ to reach the convergence of $1\ \text{cm}^{-1}$, which means including about $M_B^{\text{vib}} = 8000$ vibrational levels. Then, the corresponding rotational contribution may include up to $J^{\max} = 100$. This situation is common in the ExoMol project [85], which computes spectra of hot molecules. This leads to a set of ro-vibrational Hamiltonian matrices with the dimensions $M_B^{(\text{rv})}$ ranging from 8000 to $8000 \times (2J^{\max} + 1) = 1{,}608{,}000$.

In the following, we show how to exploit the advantages of the special structure of the ro-vibrational Hamiltonian matrix in order to simplify this problem. For large polyatomic molecules, the ro-vibrational Hamiltonian matrix has a pronounced quasi-block character built around vibrational states. This is due to the fact, see Appendix, that the off-diagonal elements $H^J_{\lambda k,\lambda' k'}$ between two different vibrational states λ and λ' always contribute substantially less to the calculated energy levels than the off-diagonal elements within a vibrational state, $H^J_{\lambda k,\lambda k'}$, where k is the quantum number giving the projection of J on the body-fixed z-axis ($k = -J, \ldots, J$) and λ runs over the vibrational basis set ($\lambda = 1, \ldots, M_B^{\text{vib}}$). Physically, this corresponds to small Coriolis interactions between different vibrational states, which is achieved by the use of the Eckart embedding [86].

Figure 3 illustrates the structure of the ro-vibrational matrix for the first four vibrational states of molecules HNO_3 ($\lambda = 1, \ldots, 4$). We can see that most of the off-diagonal $H^J_{\lambda k,\lambda' k'}$ elements are zero when $|k - k'| > 2$ reflecting the quadratic differential form of the kinetic energy operator. It can also be seen that the non-zero off-diagonal elements gather near the main diagonal, and the matrix has an almost tridiagonal form. The near-diagonal elements $H^J_{\lambda k,\lambda k'}$ are mostly associated with changes in the effective geometry of the rotating molecule through interactions with the corresponding vibrational state λ. The off-diagonal elements $H^J_{\lambda k,\lambda' k'}$ are associated with Coriolis coupling between vibrational states λ and λ'.

Importantly, the contribution of the off-diagonal elements $H^J_{\lambda k,\lambda' k'}$ corresponding to the coupling between different vibrational states is much smaller than that of the off-diagonal elements $H^J_{\lambda k,\lambda k'}$ belonging to the same vibrational state, because of the large energy separation between vibrational levels. This is illustrated in Figure 3, where the actual contributions from the off-diagonal matrix elements to the final ro-vibrational energy levels for molecules HNO_3 are

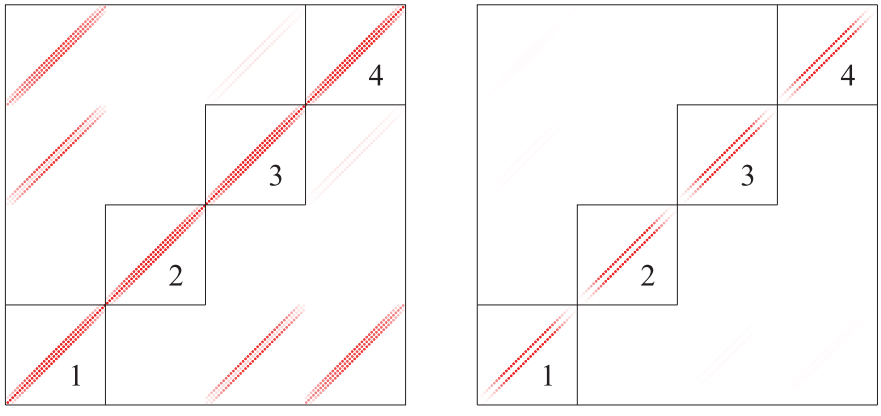

Figure 3. A: structure of the ro-vibrational matrix of HNO_3 for the first four vibrational states, $J = 20$ (the density of red is proportional to the magnitude of the individual matrix element); B: the contributions from the off-diagonal elements to the final energy levels (the density of red is proportional to the magnitude of the corresponding contribution). The squares along the diagonal depict the pure rotational sub-matrices for vibrational states $\lambda = 1, 2, 3, 4$, respectively.

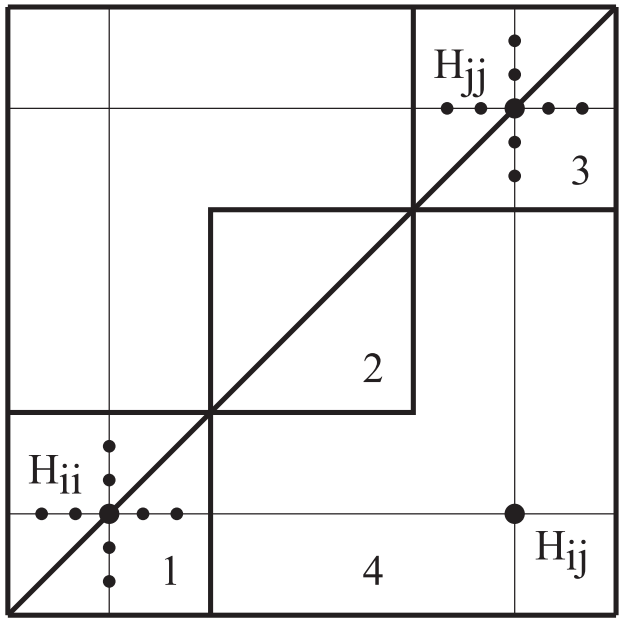

Figure 4. Hybrid scheme for partitioning of ro-vibrational Hamiltonian matrix: blocks 1, 2, and 3 correspond to different vibrational states λ; the off-diagonal matrix elements from Region 4 are generally smaller and treated using the perturbation theory. Note that indices i and j are denoted (λk) and $(\lambda' k')$, respectively, in the text which distinguished between vibrational and rotational basis functions.

shown. Typically, contribution from off-diagonal elements corresponding to different vibrational states is very small, i.e. less than 0.001 cm^{-1}.

This feature of the vibrational–rotational Hamiltonian matrix is common for large molecules and underpins the ro-vibrational version of our hybrid approach, which is schematically represented in Figure 4. Again, we use second-order perturbation theory (as defined by the Jacobi rotation) to transform the $H^J_{\lambda k,\lambda' k'}$ matrix to a block-diagonal form $\tilde{H}^J_{\lambda k,\lambda k'}$ built from rotational sub-matrices corresponding to different vibrational states λ. Thus, the dimension of each degenerate rotational sub-block is $(2J+1)$ only and we only consider M_B^{target} sub-matrices that correspond to M_B^{target} vibrational states. In the case of strong resonances between different vibrational states, these states can be combined into one, enlarged sub-matrix and treated together, i.e. for an L-fold symmetry vibrational degeneracy, the dimension of the sub-block is $L \times (2J+1)$. For details, see Appendix.

As above, we employ a single Jacobi rotation which we apply to the (complex) ro-vibrational Hermitian matrix. Our calculations show that, in contrast to the pure vibrational perturbation method, the best agreement with the variational solution is achieved when both the diagonal and off-diagonal elements are updated as given by

$$\tilde{H}^J_{\lambda k,\lambda k} = H^J_{\lambda k,\lambda k} + \sum_{\lambda' \in M_B^{\text{vib}},\lambda' \neq \lambda} \sum_{k'} t_{\lambda k,\lambda' k'} \eta_{\lambda k,\lambda' k'} \qquad (10)$$

for the diagonal elements

$$\tilde{H}^J_{\lambda k,\lambda k''} = \frac{1}{2} \sum_{\lambda' \in M_B^{\text{vib}},\lambda' \neq \lambda} \sum_{k'} \times \left[c_{\lambda k,\lambda' k'} H^J_{\lambda k,\lambda k''} + c_{\lambda k'',\lambda' k'} H^{*J}_{\lambda k,\lambda k''} + s_{\lambda k,\lambda' k'} H^J_{\lambda' k',\lambda k''} + H^J_{\lambda k,\lambda' k'} s_{\lambda' k',\lambda k''} \right], \qquad (11)$$

and for the off-diagonal elements, where

$$c_{\lambda k,\lambda' k'} = \frac{1}{\sqrt{1+t^2_{\lambda k,\lambda' k'}}},$$

$$s_{\lambda k,\lambda' k'} = \frac{c_{\lambda k,\lambda' k'} t_{\lambda k,\lambda' k'}}{\eta_{\lambda k,\lambda' k'}} H^J_{\lambda k,\lambda' k'},$$

$$t_{\lambda k,\lambda' k'} = \text{sign}(\vartheta_{\lambda k,\lambda' k'}) / \left(|\vartheta_{\lambda k,\lambda' k'}| + \sqrt{1+\vartheta^2_{\lambda k,\lambda' k'}} \right),$$

$$\eta_{\lambda k,\lambda' k'} = \text{sign}\left[\mathbb{R}\text{e}\left(H^J_{\lambda k,\lambda' k'} \right) \right] \left| H^J_{\lambda k,\lambda' k'} \right|,$$

$$\vartheta_{\lambda k,\lambda' k'} = \frac{H^J_{\lambda k,\lambda k} - H^J_{\lambda' k',\lambda' k'}}{2\eta_{\lambda k,\lambda' k'}}.$$

Here $\underline{H}^J$ and $\underline{\tilde{H}}^J$ are the initial (unperturbed) matrix and perturbed matrix, respectively; λ runs from 1 to M_B^{target}, and $k = -J, \ldots, +J$.

Equation (11) is a symmetrised version of the standard formula for the single Jacobi rotation with respect to indices λk and $\lambda k''$. It should be noted that in the limit $|H^J_{\lambda k,\lambda' k'}| \ll |H^J_{\lambda k,\lambda k} - H^J_{\lambda' k',\lambda' k'}|$, Equation (11) is identical with the corresponding expression for second-order perturbation theory:

$$\tilde{H}^J_{\lambda k,\lambda k''} = H^J_{\lambda k,\lambda k''} + \frac{1}{2} \sum_{\lambda' \in M_B^{\text{vib}},\lambda' \neq \lambda} \sum_{k'} \times \left(\frac{H^J_{\lambda k,\lambda' k'} H^{*J}_{\lambda' k',\lambda k''}}{H^J_{\lambda k,\lambda k} - H^J_{\lambda' k',\lambda' k'}} + \frac{H^J_{\lambda k,\lambda' k'} H^{*J}_{\lambda' k',\lambda k''}}{H^J_{\lambda k'',\lambda k''} - H^J_{\lambda' k',\lambda' k'}} \right). \qquad (12)$$

The resulting block-diagonal form is then diagonalised for each λ sub-matrix separately, where λ indicates either a single vibrational state or a set of strongly interacting vibrational states. Thus, our algorithm replaces the diagonalisation of a huge $[M_B^{\text{vib}} \times (2J+1)]$ ro-vibrational matrix with a number of diagonalisations of much smaller $[(2J+1)$ or $L \times (2J+1)]$ matrices, where L is the number of resonance sub-states. It should be noted that in our algorithm, the ro-vibrational wave functions, in contrast to those from an exact diagonalisation, do not contain any contribution from other vibrational states. This leads to some errors in the subsequent calculation of the transition dipole moments and intensities of the ro-vibrational transitions [87]. However, the relative error is rather small for the stronger and most important transitions because of the relatively small

perturbation contribution from the off-diagonal ($\lambda \neq \lambda'$) matrix elements $H^J_{\lambda k,\lambda' k'}$. For other states, where intensity stealing is important [88], the resonant-coupled vibrational states procedure can be used [10]. Finally, we note that our procedure is both very quick and easily parallelised.

5. Transition intensities

Although the calculation of the ro-vibrational energy levels and wave functions may be long, it is only an intermediate stage. The final step is the calculation of transition intensities which involves computing matrix elements of the dipole moment functions between the computed ro-vibrational wave functions. For hot molecules, where a huge number of transition dipoles must be evaluated, this step becomes very time consuming and even prohibitively expensive [89].

Thus, even for HNO_3, the problem of calculating the vibrational–rotational spectrum in the range of 0–4500 cm^{-1}, using a standard variational method without approximations, is extremely difficult using the existing computers. For larger molecules, such calculations are currently almost impossible.

The separable form of our hybrid rotational–vibrational wave functions, which are obtained in separate diagonalisations for each vibrational state, allows a speed-up, by several orders of magnitude, of the subsequent evaluation of transition intensities. This is because the wave functions are much more compact and represented by a number of independent parts. As we will show below, this approximation, in the case of HNO_3 and H_2O, leads to relatively small errors in the overall shape and magnitude of the ro-vibrational spectra computed at room or higher temperatures.

6. Results

Tables 5 and 6 show the pure rotational energy levels of H_2O and HNO_3 for several J values obtained using three different methods to find eigensolutions of the corresponding Hamiltonian matrices: full diagionalisation (F), the hybrid ro-vibrational approach described above (H), and a rigid-rotor calculation represented by separate diagonalisations of the rotational sub-blocks with the off-diagonal couplings with other vibrational states neglected (R).

The results for water, Table 5, are of interest because the molecule exhibits relatively large off-diagonal elements $H^J_{\lambda k,\lambda' k'}$ and thus large centrifugal effects.

The difference $\Delta\tilde{E}^{\mathrm{F-R}} = \tilde{E}^{\mathrm{F}} - \tilde{E}^{\mathrm{R}}$ illustrates the magnitude of the centrifugal and Coriolis contributions, while $\Delta\tilde{E}^{\mathrm{F-H}} = \tilde{E}^{\mathrm{F}} - \tilde{E}^{\mathrm{H}}$ shows the quality of our hybrid method for different J. For example, for $J = 1$, the maximum value of $\Delta\tilde{E}^{\mathrm{F-R}}$ is only 0.03 cm^{-1} and $\Delta\tilde{E}^{\mathrm{F-H}}$ is within 0.005 cm^{-1} and for $J = 3$, $\Delta\tilde{E}^{\mathrm{F-R}}$ is within 0.6 cm^{-1} and $\Delta\tilde{E}^{\mathrm{F-H}}$ is within 0.05 cm^{-1}. At higher J, these residuals grow significantly, up to 161 and 44 cm^{-1}, respectively, for $J = 10$.

For a given J, both $\Delta\tilde{E}^{\mathrm{F-R}}$ and $\Delta\tilde{E}^{\mathrm{F-H}}$ increase with increasing rotational energy. For example, for $J = 8$ for the lowest term value of 741.25 cm^{-1} ($K_A = 8$), $\Delta\tilde{E}^{\mathrm{F-R}} = 2.05$ cm^{-1} and $\Delta\tilde{E}^{\mathrm{F-H}} = 0.02$ cm^{-1}, while for the highest term

Table 5. Calculated values of the rotational energy levels (in cm^{-1}) for the vibrational ground state of H_2O obtained using different methods of diagonalising the Hamiltonian matrix.

$J=1$			$J=3$			$J=6$			$J=8$			$J=10$		
Full	Hybrid	Separate	Full	Hybrid	Separate	Full	Hybrid	Separate	Full	Hybrid	Separate	Full	Hybrid	Separate
23.78	23.78	23.78	136.48	136.46	136.63	445.16	445.15	446.05	741.25	741.27	743.30	1110.10	1110.17	1114.25
37.01	37.01	37.04	141.84	141.86	141.94	445.67	445.68	446.51	741.34	741.36	743.36	1110.12	1110.19	1114.25
42.33	42.33	42.34	173.41	173.38	173.57	542.57	542.37	544.34	881.59	881.57	885.35	1290.45	1290.80	1297.35
			206.00	206.05	206.32	552.11	552.21	553.51	884.06	884.21	887.50	1290.99	1291.38	1297.73
			212.04	212.07	212.38	603.25	603.00	605.72	983.49	983.38	989.97	1437.91	1438.88	1449.77
			285.02	284.97	286.59	648.63	649.02	651.08	1005.67	1006.26	1011.01	1445.39	1446.60	1456.00
			285.23	285.18	286.80	661.79	662.03	664.64	1051.46	1051.91	1059.19	1540.49	1542.89	1557.39
						756.87	757.49	761.98	1122.96	1124.40	1130.72	1582.01	1584.84	1596.30
						757.99	758.61	763.12	1132.61	1134.11	1141.04	1619.15	1623.20	1637.39
						890.14	890.12	901.68	1256.47	1258.37	1269.40	1720.48	1724.91	1739.20
						890.18	890.15	901.71	1257.27	1259.21	1270.23	1726.95	1731.94	1746.51
						1049.72	1046.94	1073.55	1415.37	1416.12	1439.06	1878.59	1883.34	1906.06
						1049.72	1046.94	1073.55	1415.40	1416.16	1439.09	1879.12	1883.97	1906.63
									1599.11	1595.54	1641.45	2061.68	2064.15	2105.58
									1599.11	1595.54	1641.45	2061.70	2064.19	2105.60
									1805.18	1791.73	1876.13	2267.96	2263.69	2338.32
									1805.18	1791.73	1876.13	2267.96	2263.69	2338.32
												2494.83	2476.44	2603.63
												2494.83	2476.44	2603.63
												2740.26	2696.06	2901.09
												2740.26	2696.06	2901.09

Table 6. Calculated values of the rotational energy levels (in cm^{-1}) for the vibrational ground state of HNO_3 obtained using different methods of diagonalising the Hamiltonian matrix.

$J = 1$			$J = 10$			$J = 15$			$J = 45$			$J = 60$		
Full	Hybrid	Separate	Full	Hybrid	Separate	Full	Hybrid	Separate	Full	Hybrid	Separate	Full	Hybrid	Separate
0.61	0.61	0.61	53.18	53.18	53.18	200.17	200.17	200.21	440.89	440.89	441.09	775.20	775.19	775.81
0.64	0.64	0.64	59.24	59.24	59.24	212.49	212.49	212.54	477.62	477.62	477.86	824.40	824.40	825.12
0.84	0.84	0.84	64.88	64.88	64.88	224.39	224.39	224.45	512.65	512.65	512.96	871.90	871.90	872.76
			70.09	70.09	70.10	246.93	246.93	247.01	545.98	545.98	546.38	917.69	917.69	918.72
			74.89	74.89	74.90	257.56	257.56	257.66	577.63	577.63	578.12	961.77	961.77	963.00
			79.27	79.27	79.28	267.78	267.78	267.89	607.58	607.58	608.18	1004.15	1004.14	1005.60
			83.22	83.22	83.23	286.94	286.94	287.09	635.84	635.84	636.56	1044.82	1044.82	1046.52
			86.74	86.74	86.76	295.89	295.89	296.06	662.41	662.41	663.25	1083.80	1083.80	1085.76
			89.83	89.83	89.85	304.42	304.42	304.60	687.29	687.28	688.26	1121.08	1121.08	1123.32
			92.48	92.48	92.50	320.20	320.20	320.42	710.47	710.47	711.57	1156.67	1156.66	1159.19
			94.62	94.62	94.64	327.45	327.45	327.69	731.95	731.94	733.18	1190.56	1190.55	1193.38
			96.09	96.09	96.12	334.28	334.28	334.54	751.73	751.71	753.08	1222.76	1222.74	1225.87
			97.16	97.16	97.19	346.64	346.64	346.94	769.77	769.76	771.25	1253.26	1253.24	1256.67
			98.54	98.55	98.57	352.17	352.16	352.48	786.07	786.05	787.67	1282.06	1282.03	1285.77
			100.47	100.47	100.49	357.25	357.24	357.58	800.58	800.53	802.29	1309.15	1309.11	1313.16
			102.76	102.75	102.78	366.00	365.98	366.37	813.21	813.13	815.03	1334.53	1334.48	1338.84
						369.57	369.52	369.96	823.70	823.48	825.65	1358.19	1358.12	1362.78
						372.34	372.25	372.76	830.85	830.33	832.97	1380.09	1380.01	1384.97
						376.42	376.42	376.83	837.09	837.27	839.13	1400.23	1400.12	1405.39
						379.27	379.36	379.67	846.55	847.12	848.51	1418.54	1418.38	1423.97
						382.75	382.88	383.15	857.83	858.41	859.73	1434.96	1434.71	1440.65
						390.87	390.93	391.24	870.48	870.69	872.29	1449.30	1448.86	1455.28
						395.40	395.35	395.76	884.34	883.72	886.04	1460.97	1459.67	1467.32
						400.22	400.00	400.55				1468.58	1467.55	1475.24
												1490.44	1492.11	1496.62
												1520.79	1522.31	1526.63
												1556.46	1555.09	1561.82

value 1805.18 cm^{-1} ($K_A = 0$), we obtain $\Delta\tilde{E}^{F-R} = 71.0$ cm^{-1} and $\Delta\tilde{E}^{F-H} = 13.4$ cm^{-1}.

Thus, we conclude that for a small molecule with large centrifugal effects, like water, the hybrid method does not provide accurate ro-vibrational energies. Indeed, it is well known that the $J = 0$ contraction performs poorly for water [90] because of issues with linear geometry. However, for such systems purely variational calculations do not present a computational problem [91]. For larger molecules, it is generally not necessary to deal with issues associated with quasi-linearity.

For larger molecules with smaller rotational constants, centrifugal distortion effects are expected to decrease significantly. Therefore, we also expect the hybrid method to perform better for such systems. Tables 6 illustrates this effect for HNO_3. For example, for $J = 60$ for the maximal residuals, we obtain $\Delta\tilde{E}^{F-R} = 5.63$ cm^{-1} and $\Delta\tilde{E}^{F-H} = 1.35$ cm^{-1}, which also correspond to the highest term value 1556.46 cm^{-1} for the $J = 60$ manifold ($K_A = 0$). For the rotational levels in the range $1 \leq J \leq 60$, the average error of the hybrid method is within 0.02 cm^{-1}, i.e. much better than that for water for the same energy range. The range $J \leq 60$ is selected as it represents the states which are important for the room-temperature ro-vibrational spectrum of HNO_3. It should be noted that for large molecules with small rotational constants, like HNO_3, individual absorption lines are often not resolved because of the high density of the lines even at room temperature. For example, the spectrum of HNO_3 contains 2×10^{10} lines in the region 0–4000 cm^{-1} with intensities above 10^{-27} cm/molecules at 600 K. This suggests that calculations with the accuracy within 0.02 cm^{-1} should be sufficient for most purposes.

As an example, Figure 5 shows the absorption cross-sections calculated in the region of the ν_3 and ν_4 bands of HNO_3 for $T = 298$ K using the full variational ('Full') calculation as well as the difference with the hybrid calculation. Here a Voigt line profile was used with parameters $\sigma = \gamma = 0.075$ cm^{-1} (a half width at half maximum (HWHM) of 0.153 cm^{-1}), chosen to match spectra from the PNNL database [92]. Further details of these spectra will be given elsewhere [80]. For the central part of the band ($J < 40$), where the rotational lines are strong enough to be resolved, the two methods (full and hybrid) give almost identical results. At the edges of the bands ($40 \leq J \leq 60$), slight differences in the frequencies and intensities of the individual ro-vibrational absorption lines appear. However, the rotational structure is poorly resolved due to superposition of a large number of lines. Besides the intensity of the band

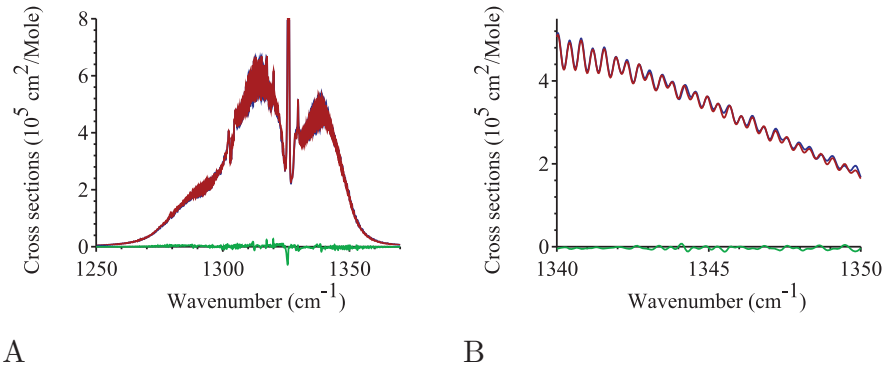

Figure 5. Absorption spectrum of HNO_3 calculated using the full diagonalisation of the ro-vibrational Hamiltonian matrix (red curve), and our hybrid method (blue curve). The green curve gives the difference between these two methods. A: ν_3 and ν_4 bands; B: *P*-branch of the ν_3 band.

diminishes rapidly with J due to the decreasing population of the highly excited rotational levels; therefore, the absolute difference is also negligible.

7. Conclusion

In this paper, two hybrid variational–perturbation methods for computing vibration and ro-vibrational energies for large molecules are proposed. These methods yield significant speed-ups for the computation of ro-vibrational spectra, with only a minor loss of accuracy, at least for semi-rigid polyatomic molecules. We plan to use method to compute extensive line lists and cross sections for large molecules, including nitric acid [93], as part of the ExoMol project [85].

As an illustration of the efficiency of the hybrid method, calculations of the vibrational and ro-vibrational energies of a tri- and a penta-atomic molecule are presented. We can use these to project to even larger systems. Assuming that it is currently feasible to diagonalise a matrix of about 1,000,000 by 1,000,000 and using Equation (5), we can expect to achieve an accuracy of 1 cm^{-1} for all ro-vibrational term values for polyads $N_V \leq 4$ for a given potential energy surface for a molecule containing up to 15 atoms using our hybrid procedure. For molecules containing up to 25 atoms, the expected accuracy is about 5 cm^{-1}.

Our hybrid methods have several advantages:

(1) They are relatively easy to implement as an extension to a pure variational computer program, which readily provides all required components. For example, all the calculations presented here were performed using ANGMOL [74], a variational program for ro-vibrational spectra of general polyatomic molecules. It required changes to less than 1% of the entire program to implement the hybrid methods.
(2) They allow efficient parallelisation and vectorisation of the code.
(3) They are very fast compared to full diagonalisation. Not only is the diagonalisation time greatly reduced, but also only a small proportion of the Hamiltonian matrices needs to be computed. Furthermore, the coupling elements can be evaluated on the fly and do not need to be stored in the memory.
(4) Our method adopts several approximations arising from second-order perturbation theory and the rigid rotor model to full diagonalisation approaching the variational limit. For the vibration-only problem, this approximation is easily controlled by altering the size of the block 1.

Our method has scope for further improvement. For example:

- For the purely vibrational Hamiltonian matrix, one can change not only the diagonal but also the off-diagonal elements in block 1, as we do for the ro-vibrational Hamiltonian matrix. This will increase the accuracy at the expense of increased computer time.
- One could use not only one but two or more consecutive Jacobi rotations. Again, this will increase the accuracy at the expense of increased computer time.
- Simple perturbation theory corrections generally overestimate the effect of the perturbation. One could reduce this effect by multiplying the computed perturbations by some empirical coefficient $0 < p \leq 1$. This will increase the accuracy without increasing the computer time. The problem with this approach is that the magnitude of p depends on the number of degrees-of-freedom involved, the structure and size of the Hamiltonian matrix, and value of perturbation adjustment.
- Finally, we note that in our present implementation, no advantage is taken of the pronounced polyad structure shown by many molecules. This could be

achieved by a suitable choice of the $\underline{\alpha}$ coefficients in Equation (4).

Funding

This work was supported by the ERC under Advanced Investigator Project [grant number 267219].

References

[1] J.H. Van Vleck, Phys. Rev. **33**, 467 (1929).
[2] O.M. Jordahl, Phys. Rev. **45**, 87 (1934).
[3] W.H. Shaffer, H.H. Nielsen, and L.H. Thomas, Phys. Rev. **56**, 895 (1939).
[4] H.H. Nielsen, Rev. Mod. Phys. **23**, 90 (1951).
[5] C. Bloch, Nucl. Phys. **6**, 329 (1958).
[6] C.T.G. Amat and H.H. Nielsen, *Rotation-Vibration of Polyatomic Molecules* (Dekker, New York, 1971).
[7] F. Jørgensen and T. Pedersen, Mol. Phys. **27**, 33 (1974).
[8] S. Califano, *Vibrational States* (John Wilay and Sons, New York, London, 1976).
[9] V.G. Tyuterev and V.I. Perevalov, Chem. Phys. Lett. **74**, 494 (1980).
[10] D.J. Klein, J. Chem. Phys. **61**, 786 (1974).
[11] I.M. Mills, J. Mol. Spectrosc. **5**, 334 (1961).
[12] I.M. Mills, J. Mol. Spectrosc. **17**, 164 (1965).
[13] V. Barone, J. Chem. Phys. **122**, 014108 (2005).
[14] V. Barone, J. Bloino, C.A. Guido, and F. Lipparini, Chem. Phys. Lett. **496**, 157 (2010).
[15] L.A. Gribov, Opt. Spectrosc **31**, 456 (1971).
[16] I. Suzuky, Bull. Chem Soc. Japan **44**, 3277 (1971).
[17] M.G. Bucknell, N.C. Handy, and S.F. Boys, Mol. Phys. **28**, 759 (1974).
[18] M.G. Bucknell and N.C. Handy, Mol. Phys. **28**, 777 (1974).
[19] R.J. Whitehead and N.C. Handy, J. Mol. Spectrosc. **55**, 356 (1975).
[20] G.D. Carney and C.W. Kern, Int. J. Quantum Chem. **S9**, 317 (1975).
[21] R.J. Whitehead and N.C. Handy, J. Mol. Spectrosc. **59**, 459 (1976).
[22] G.D. Carney and R.N. Porter, J. Chem. Phys. **65**, 3547 (1976).
[23] G.D. Carney, S.R. Langhoff, and L.A. Curtiss, J. Chem. Phys. **66**, 3724 (1977).
[24] G.D. Carney and R.N. Porter, Chem. Phys. Lett. **50**, 327 (1977).
[25] G.D. Carney, S. Giorgianni, and K.N. Rao, J. Mol. Spectrosc. **80**, 158 (1980).
[26] G.D. Carney and R.N. Porter, Phys. Rev. Lett. **45**, 537 (1980).
[27] S. Carter and N.C. Handy, Mol. Phys. **47**, 1445 (1982).
[28] J. Tennyson and B.T. Sutcliffe, J. Chem. Phys. **77**, 4061 (1982).
[29] G. Brocks and J. Tennyson, J. Mol. Spectrosc. **99**, 263 (1983).
[30] S. Carter, N. Handy, and B.T. Sutcliffe, Mol. Phys. **49**, 745 (1983).
[31] J. Tennyson and B.T. Sutcliffe, J. Chem. Phys. **79**, 43 (1983).
[32] D. Cropek and G.D. Carney, J. Chem. Phys. **80**, 4280 (1984).
[33] J. Tennyson and B.T. Sutcliffe, Mol. Phys. **51**, 887 (1984).
[34] J. Tennyson, Comput. Phys. Commun. **29**, 307 (1983).
[35] J. Tennyson, Comput. Phys. Commun. **42**, 257 (1986).
[36] J. Tennyson and S. Miller, Comput. Phys. Commun. **55**, 149 (1989).
[37] S. Carter, P. Rosmus, N.C. Handy, S. Miller, J. Tennyson, and B.T. Sutcliffe, Comput. Phys. Commun. **55**, 71 (1989).
[38] J.C. Light, I.P. Hamilton, and J.V. Lill, J. Chem. Phys. **82**, 1400 (1985).
[39] Z. Bačić and J.C. Light, Annu. Rev. Phys. Chem. **40**, 469 (1989).
[40] J.C. Light and T. Carrington Jr, ,Adv. Phys. Chem. **114**, 263 (2000).
[41] I.N. Kozin, M.M. Law, J. Tennyson, and J.M. Hutson, Comput. Phys. Commun. **163**, 117 (2004).
[42] S.N. Yurchenko, W. Thiel, and P. Jensen, J. Mol. Spectrosc. **245**, 126 (2007).
[43] P. Botschwina, Chem. Phys. **40**, 33 (1979).
[44] P. Botschwina, H. Haertner, and W. Sawodny, Chem. Phys. Lett. **74**, 156 (1980).
[45] P. Botschwina, Chem. Phys. **68**, 41 (1982).
[46] P. Botschwina, Chem. Phys. **81**, 73 (1983).
[47] P. Botschwina and P. Sebald, J. Mol. Spectrosc. **100**, 1 (1983).
[48] Y.I. Ponomarev and A.I. Pavlyuchko, Opt. I Spektrosk. **44**, 1262 (1978).
[49] G.V. Yukhnevich, E.G. Kokhanova, A.I. Pavlyuchko, and V.V. Volkov, J. Mol. Struct. (THEOCHEM) **23**, 1 (1985).
[50] A.I. Pavlyuchko and L.A. Gribov, Opt. I Spektrosk. **58**, 1247 (1985).
[51] A.I. Pavlyuchko, Opt. I Spektrosk. **67**, 286 (1989).
[52] A.I. Pavlyuchko, J. Struct. Chem. **36**, 204 (1995).
[53] A.I. Pavlyuchko, J. Struct. Chem. **36**, 210 (1995).
[54] A.I. Pavlyuchko, J. Struct. Chem. **38**, 959 (1997).
[55] A.A. Vigasin, F. Huisken, A.I. Pavlyuchko, L. Ramonat, and E.G. Tarakanova, J. Mol. Spectrosc. **209**, 81 (2001).
[56] A.A. Vigasin, A.I. Pavlyuchko, Y. Jin, and S. Ikawa, J. Mol. Struct. **742**, 173 (2005).
[57] A.I. Pavlyuchko and L.A. Gribov, J. Struct. Chem. **51**, 444 (2010).
[58] M. Pavanello, L. Adamowicz, A. Alijah, N.F. Zobov, I.I. Mizus, O.L. Polyansky, J. Tennyson, T. Szidarovszky, A.G. Császár, M. Berg, A. Petrignani, and A. Wolf, Phys. Rev. Lett. **108**, 023002 (2012).
[59] J. Tennyson and B.T. Sutcliffe, Mol. Phys. **58**, 1067 (1986).
[60] S. Miller and J. Tennyson, Chem. Phys. Lett. **145**, 117 (1988).
[61] H.Y. Mussa and J. Tennyson, J. Chem. Phys. **109**, 10885 (1998).
[62] R.B. Gerber and M.A. Ratner, Chem. Phys. Lett. **68**, 195 (1979).
[63] J.M. Bowman, Acc. Chem. Res. **19**, 202 (1986).
[64] R.B. Gerber and M.A. Ratner, Adv. Chem. Phys. **70**, 97 (1988).
[65] S. Carter, J.M. Bowman, and N.C. Handy, Theor. Chem. Acc. **100**, 191 (1998).
[66] N.C. Handy and S. Carter, Mol. Phys. **102**, 2201 (2004).
[67] Y. Scribano and D.M. Benoit, Chem. Phys. Lett. **458**, 384 (2008).
[68] Y. Scribano, D.M. Lauvergnat, and D.M. Benoit, J. Chem. Phys. **133**, 094103 (2010).
[69] J.M. Bowman, S. Carter, and X.C. Huang, Int. J. Quantum Chem. **22**, 533 (2003).
[70] M.L. Senent, P. Palmieri, S. Carter, and N.C. Handy, Chem. Phys. Lett. **354**, 1 (2002).
[71] C. Fabri, T. Furtenbacher, and A.G. Császár, Mol. Phys. **112**, 2462 (2014).
[72] E. Mátyus, G. Czakó, B.T. Sutcliffe, and A.G. Császár, J. Chem. Phys. **127**, 084102 (2007).
[73] J.K.G. Watson, Mol. Phys. **15**, 479 (1968).

[74] L.A. Gribov and A.I. Pavlyuchko, *Variational Methods for Solving Anharmonic Problems in the Theory of Vibrational Spectra of Molecules* (Nauka, Moscow, 1998), (in Russian).
[75] G.O. Sørensen, in *Topics in Current Chemistry*, edited by M.J.S. Dewar et al, Vol. 82 (Springer-Verlag, Dordrecht, 1979), 99 p.
[76] S.N. Yurchenko, W. Thiel, and P. Jensen, J. Mol. Spectrosc. **245**, 126 (2007).
[77] F. Gatti and C. Iung, Phys. Rep. **484**, 1 (2009).
[78] J. Tennyson, P.F. Bernath, L.R. Brown, A. Campargue, M.R. Carleer, A.G. Császár, L. Daumont, R.R. Gamache, J.T. Hodges, O.V. Naumenko, O.L. Polyansky, L.S. Rothmam, A.C. Vandaele, N.F. Zobov, A.R. Al Derzi, C. Fábri, A.Z. Fazliev, T. Furtenbacher, I.E. Gordon, L. Lodi, and I.I. Mizus, J. Quant. Spectrosc. Radiat. Transf. **117**, 29 (2013).
[79] L.S. Rothman, I.E. Gordon, Y. Babikov, A. Barbe, D.C. Benner, P.F. Bernath, M. Birk, L. Bizzocchi, V. Boudon, L.R. Brown, A. Campargue, K. Chance, E.A. Cohen, L.H. Coudert, V.M. Devi, B.J. Drouin, A. Fayt, J.M. Flaud, R.R. Gamache, J.J. Harrison, J.M. Hartmann, C. Hill, J.T. Hodges, D. Jacquemart, A. Jolly, J. Lamouroux, R.J. Le Roy, G. Li, D.A. Long, O.M. Lyulin, C.J. Mackie, S.T. Massie, S. Mikhailenko, H.S.P. Müller, O.V. Naumenko, A.V. Nikitin, J. Orphal, V. Perevalov, A. Perrin, E.R. Polovtseva, C. Richard, M.A.H. Smith, E. Starikova, K. Sung, S. Tashkun, J. Tennyson, G.C. Toon, V.G. Tyuterev, and G. Wagner, J. Quant. Spectrosc. Radiat. Transf. **130**, 4 (2013).
[80] A.I. Pavlyuchko, S.N. Yurchenko, and J. Tennyson, J. Chem. Phys. (2014), (submitted).
[81] C.G.J. Jacobi, Crelle's J. **30**, 51 (1846), (in German).
[82] J.H. Wilkinson, *The Algebraic Eigenvalue Problem* (Oxford University Press, Oxford, 1965).
[83] K.J. Feierabend, D.K. Havey, M.E. Varner, J.F. Stanton, and V. Vaida, J. Chem. Phys. **124**, 124323 (2006).
[84] S.N. Yurchenko, R.J. Barber, A. Yachmenev, W. Thiel, P. Jensen, and J. Tennyson, J. Phys. Chem. A **113**, 11845 (2009).
[85] J. Tennyson and S.N. Yurchenko, Mon. Not. R. Astron. Soc. **425**, 21 (2012).
[86] C. Eckart, Phys. Rev. **47**, 552 (1935).
[87] H.H. Nielsen, Int. J. Quantum Chem. **1**, 217 (1967).
[88] S. Miller, J. Tennyson, and B.T. Sutcliffe, J. Mol. Spectrosc. **141**, 104 (1990).
[89] S.N. Yurchenko and J. Tennyson, Mon. Not. R. Astron. Soc. **440**, 1649 (2014).
[90] J.C. Light, R.M. Whitnell, T.J. Pack, and S.E. Choi, in *Supercomputer Algorithms for Reactivity, Dynamics and Kinetics of Small Molecules*, edited by A. Laganà, *NATO ASI Series C*, Vol. 277 (Kluwer, Dordrecht, 1989), 187p.
[91] R.J. Barber, J. Tennyson, G.J. Harris, and R.N. Tolchenov, Mon. Not. R. Astron. Soc. **368**, 1087 (2006).
[92] S.W. Sharpe, T.J. Johnson, R.L. Sams, P.M. Chu, G.C. Rhoderick, and P.A. Johnson, Appl. Spectrosc. **58**, 1452 (2004).
[93] A.I. Pavlyuchko, A. Yachmenev, J. Tennyson, and S.N. Yurchenko 2014, (work in progress).

Appendix. The Hamiltonian

Our rotational–vibrational Hamiltonian written in curvilinear internal coordinates and an Eckart embedding has the following form [74]:

$$\hat{H}_{vr} = \hat{H}_v - \frac{\hbar^2}{2}\sum_{a,b}\frac{\partial}{\partial\xi_a}\mu_{ab}(\underline{q})\frac{\partial}{\partial\xi_b}, \xi_a, \xi_b = \alpha, \beta, \gamma, \quad \text{(A1)}$$

where $\underline{\xi}$ are the rotational coordinates and $\hat{H}_v$ is the vibrational part of the Hamiltonian

$$\hat{H}_v = \hat{T}_v + V(\underline{q}) \quad \text{(A2)}$$

$$\hat{T}_v = -\frac{\hbar^2}{2}\sum_{i,j} t^{\frac{1}{4}}\frac{\partial}{\partial q_i}g_{ij}(\underline{q})t^{-\frac{1}{2}}\frac{\partial}{\partial q_j}t^{\frac{1}{4}}. \quad \text{(A3)}$$

Here q_i are internal, vibrational curvilinear coordinates given by changes in bond lengths or changes in the valence bond angles, dihedral angles, etc.; α, β, and γ are the Euler angles between the axes of the equilibrium moment of inertia tensor and external Cartesian coordinate axes; $\mu_{ab}(\underline{q})$ are elements of the inverse of the moment of inertia tensor, $\underline{I}(\underline{q})$; $\hat{T}_v$ is the vibrational kinetic energy operator and $g_{ij}(\underline{q})$ are elements of the kinetic energy coefficients matrix $\underline{G}(\underline{q})$ and $t = \det[\underline{G}]$. Finally, $V(\underline{q})$ is the molecular potential energy.

After transformation, the vibrational kinetic operator can be written as

$$\hat{T}_v = -\frac{\hbar^2}{2}\sum_{i,j}\frac{\partial}{\partial q_i}g_{ij}(\underline{q})\frac{\partial}{\partial q_j} + \beta(\underline{q}), \quad \text{(A4)}$$

where

$$\beta(\underline{q}) = -\frac{\hbar^2}{2}\sum_{i,j}\left\{\frac{\partial g_{ij}(\underline{q})}{\partial q_i}\sum_{k,l}\zeta_{kl}(\underline{q})\frac{\partial g_{kl}(\underline{q})}{\partial q_j}\right.$$
$$+\frac{1}{4}g_{ij}(\underline{q})\left[\sum_{k,l}\zeta_{kl}(\underline{q})\frac{\partial^2 g_{kl}(\underline{q})}{\partial q_i\partial q_j} - \sum_{k,l,m,n}\zeta_{kl}(\underline{q})\zeta_{mn}(\underline{q})\right.$$
$$\left.\left.\times\left(\frac{\partial g_{lm}(\underline{q})}{\partial q_i}\frac{\partial g_{kn}(\underline{q})}{\partial q_j} + \frac{\partial g_{kl}(\underline{q})}{\partial q_i}\frac{\partial g_{mn}(\underline{q})}{\partial q_j}\right)\right]\right\} \quad \text{(A5)}$$

is the so-called pseudo-potential [73]; $\zeta_{ij}(\underline{q})$ are elements of $\underline{G}(\underline{q})^{-1}$.

$\underline{G}(\underline{q})$ is a complicated function of the internal coordinates, with the elements in general case given elsewhere [74]. If the coordinates associated with both indices *i* and *j* represents changes in the bond lengths, then,

$$g_{ij}(\underline{q}) = g^0_{ij}(\underline{\varphi}), \quad \text{(A6)}$$

if the coordinate *i* represents a change in the bond length and *j* is an angular coordinate, then,

$$g_{ij}(\underline{q}) = \sum_k \frac{1}{r_k}g^k_{ij}(\underline{\varphi}), \quad \text{(A7)}$$

and if *i* and *j* both represent angular coordinates, it becomes

$$g_{ij}(\underline{q}) = \sum_{k,l}\frac{1}{r_k r_l}g^{kl}_{ij}(\underline{\varphi}). \quad \text{(A8)}$$

In these expressions, r_k is the bondlength of the *k*th bond and $\underline{\varphi}$ represents the angular coordinates.

The computation of $\underline{G}(\underline{q})$ is achieved using a second-order Taylor expansion in the angular coordinates

$$g_{ij}(\underline{q}) = g^0_{ij}(0) + \sum_m \left(\frac{\partial g^0_{ij}(\underline{\varphi})}{\partial \varphi_m}\right)_0 \varphi_m + \frac{1}{2}\sum_{m,n}\left(\frac{\partial^2 g^0_{ij}(\underline{\varphi})}{\partial\varphi_m\partial\varphi_n}\right)_0 \varphi_m\varphi_n, \tag{A9}$$

$$g_{ij}(\underline{q}) = \sum_k \frac{1}{r_k}\left[g^k_{ij}(0) + \sum_m \left(\frac{\partial g^k_{ij}(\underline{\varphi})}{\partial \varphi_m}\right)_0 \varphi_m + \frac{1}{2}\sum_{m,n}\left(\frac{\partial^2 g^k_{ij}(\underline{\varphi})}{\partial\varphi_m\partial\varphi_n}\right)_0 \varphi_m\varphi_n\right], \tag{A10}$$

$$g_{ij}(\underline{q}) = \sum_{k,l} \frac{1}{r_k r_l}\left[g^{kl}_{ij}(0) + \sum_m \left(\frac{\partial g^{kl}_{ij}(\underline{\varphi})}{\partial \varphi_m}\right)_0 \varphi_m + \frac{1}{2}\sum_{m,n}\left(\frac{\partial^2 g^{kl}_{ij}(\underline{\varphi})}{\partial\varphi_m\partial\varphi_n}\right)_0 \varphi_m\varphi_n\right]. \tag{A11}$$

These formulae are exact as $g^0_{ij}(\underline{\varphi})$, $g^k_{ij}(\underline{\varphi})$, and $g^{kl}_{ij}(\underline{\varphi})$ are quadratic functions of angles when the angular coordinates. The $\underline{\varphi}$ are represented as cosine differences $\cos\varphi_i - \cos\varphi^e_i$, where $\cos\varphi^e_i$ is the instantaneous equilibrium angle for bond angles, and sine differences for dihedral angles.

To calculate the vibrational Hamiltonian matrix elements in block 2, which give the perturbative contribution to block 1, the vibrational kinetic energy coefficients are expanded in the polynomial form and truncated after the second-order

$$g_{ij}(\underline{q}) = g_{ij}(0) + \sum_m \left(\frac{\partial g_{ij}(\underline{q})}{\partial q_m}\right)_0 q_m + \frac{1}{2}\sum_{m,n}\left(\frac{\partial^2 g_{ij}(\underline{q})}{\partial q_m\partial q_n}\right)_0 q_m q_n. \tag{A12}$$

This form is convenient because it allows faster (by an order-of-magnitude or more) computation of the coefficients without significant loss of accuracy.

The potential energy function used by us is a fourth-order polynomial

$$V(\underline{q}) = \frac{1}{2}\sum_{i,j} D_{ij}x_i x_j + \frac{1}{6}\sum_{i,j,k} D_{ijk}x_i x_j x_k + \frac{1}{24}\sum_{i,j,k,l} D_{ijkl}x_i x_j x_k x_l, \tag{A13}$$

where a Morse transformation, $x_i = (1 - \exp^{-\alpha_i \Delta r_i})$, is used to represent changes in terminal bonds such as X–H and $x_i = q_i$ for angular coordinates and the coordinates of skeletal changes in the bond lengths.

In variational calculations of vibrational energy levels, the Hamiltonian matrix elements

$$H_{kn,ml} = \langle \chi_{kn}|\hat{H}_v|\chi_{ml}\rangle \tag{A14}$$

are computed using the product form

$$\chi_{kn} = \prod_i \phi_{k_i}(r_i)\prod_s \psi_{n_s}(Q_s) \tag{A15}$$

of the basis functions, which are eigenfunctions of the Morse or harmonic oscillators. Morse oscillator functions, $\phi_{k_i}(r_i)$, are used for the stretching coordinates, r_i, for which the potential is given using a Morse transformation. Harmonic basis functions, $\psi_{n_s}(Q_s)$, are used for the other coordinates which are represented using the curvilinear normal coordinates

$$Q_s = \sum_i L^{(q)}_{is} q_i \tag{A16}$$

expressed as a linear sum over the internal coordinates, q_i, for which the potential function is defined as a Taylor series. The coordinates Q_s are those which diagonalise the harmonic part of the Hamiltonian given in the internal coordinates q_i. With these definitions, all multidimensional integrals required to calculate the Hamiltonian matrix elements are separated into products of one-dimensional integrals between either Morse functions or harmonic oscillators. All these integrals have a simple analytic form which results in high-speed computation of the Hamiltonian matrix elements. Diagonalising the Hamiltonian matrix gives the anharmonic vibrational energy levels E^{vib}_λ and the corresponding wave functions $\phi^{\text{vib}}_\lambda$.

For ro-vibrational energy levels, it is necessary to calculate elements of the complex Hermitian Hamiltonian matrix

$$H^{JJ'}_{\lambda km,\lambda' k'm'} = \left\langle \chi^J_{\lambda km}\left|\hat{H}_{vr}\right|\chi^{*J'}_{\lambda' k'm'}\right\rangle, \tag{A17}$$

using the variational basis functions

$$\chi^J_{\lambda km} = \Phi^{\text{vib}}_\lambda \phi^J_{km}, \quad \phi^J_{km} = \left(\frac{2J+1}{8\pi^2}\right)^{1/2} D^{J*}_{km}, \tag{A18}$$

where D^J_{km} is a (complex) Wigner function. In this case,

$$H^{JJ'}_{\lambda km,\lambda' k'm'} = E^{\text{vib}}_\lambda \delta_{\lambda\lambda'}\delta_{JJ'}\delta_{kk'}\delta_{mm'} - \left\langle \Phi^{\text{vib}}_\lambda \phi^J_{km}\left|\frac{\hbar^2}{2}\sum_{a,b}\frac{\partial}{\partial\xi_a}\mu_{ab}(\underline{q})\frac{\partial}{\partial\xi_b}\right|\Phi^{\text{vib}}_{\lambda'}\phi^{*J'}_{k'm'}\right\rangle. \tag{A19}$$

This expression is equivalent to

$$H^{JJ'}_{\lambda km,\lambda' k'm'} = H^J_{\lambda k,\lambda' k'}\delta_{J,J'}\delta_{mm'}, \tag{A20}$$

where

$$H^J_{\lambda k,\lambda' k'} = E^{\text{vib}}_\lambda \delta_{\lambda\lambda'}\delta_{JJ'}\delta_{kk'}\delta_{mm'} - \frac{\hbar^2}{2}\sum_{a,b}\bar{\mu}^{\lambda\lambda'}_{ab}\left\langle \phi^J_{km}\left|\frac{\partial^2}{\partial\xi_a\partial\xi_b}\right|\phi^{*J}_{k'm'}\right\rangle \delta_{JJ'}\delta_{mm'}, \tag{A21}$$

and

$$\bar{\mu}^{\lambda\lambda'}_{ab} = \left\langle \Phi^{\text{vib}}_\lambda|\mu_{ab}(\underline{q})|\Phi^{\text{vib}}_{\lambda'}\right\rangle. \tag{A22}$$

To calculate $\bar{\mu}_{ab}^{\lambda\lambda'}$, the matrix elements $\mu_{ab}(\underline{q})$ are expanded to the secondorder as a Taylor series,

$$\mu_{ab}(\underline{q}) = \mu_{ab}(0) + \sum_m \left(\frac{\partial \mu_{ab}(\underline{q})}{\partial q_m}\right)_0 q_m + \frac{1}{2}\sum_{m,n}\left(\frac{\partial^2 \mu_{ab}(\underline{q})}{\partial q_m \partial q_n}\right)_0 q_m q_n, \quad \text{(A23)}$$

where

$$\left(\frac{\partial \mu_{ab}(\underline{q})}{\partial q_m}\right)_0 = -\sum_{i,j}\frac{\left(\frac{\partial I_{ij}(\underline{q})}{\partial q_m}\right)_0}{I_{ia}(0)I_{ib}(0)},$$

$$\left(\frac{\partial^2 \mu_{ab}(\underline{q})}{\partial q_m \partial q_n}\right)_0 = -\sum_{i,j}\frac{\left(\frac{\partial^2 I_{ij}(\underline{q})}{\partial q_m \partial q_n}\right)_0}{I_{ia}(0)I_{ib}(0)} + \sum_{i,j,k,l}\left[\frac{\left(\frac{\partial I_{ij}(\underline{q})}{\partial q_m}\right)_0\left(\frac{\partial I_{kl}(\underline{q})}{\partial q_n}\right)_0}{I_{ia}(0)I_{jk}(0)I_{lb}(0)} + \frac{\left(\frac{\partial I_{ij}(\underline{q})}{\partial q_m}\right)_0\left(\frac{\partial I_{kl}(\underline{q})}{\partial q_n}\right)_0}{I_{jb}(0)I_{ik}(0)I_{la}(0)}\right]. \quad \text{(A24)}$$

In this case,

$$\bar{\mu}_{ab}^{\lambda\lambda'} = \left\langle \Phi_\lambda^{\text{vib}} \right| \mu_{ab}(\underline{q}) \left| \Phi_{\lambda'}^{\text{vib}} \right\rangle = \mu_{ab}(0)\delta_{\lambda\lambda'} + \sum_m \left(\frac{\partial \mu_{ab}(\underline{q})}{\partial q_m}\right)_0 \left\langle \Phi_\lambda^{\text{vib}} \left| q_m \right| \Phi_{\lambda'}^{\text{vib}} \right\rangle + \frac{1}{2}\sum_{m,n}\left(\frac{\partial^2 \mu_{ab}(\underline{q})}{\partial q_m \partial q_n}\right)_0 \left\langle \Phi_\lambda^{\text{vib}} \left| q_m q_n \right| \Phi_{\lambda'}^{\text{vib}} \right\rangle, \quad \text{(A25)}$$

and all the integrals reduce to products of one-dimensional integrals over either Morse or harmonic oscillators.

When analysing the off-diagonal elements of the vibrational–rotational Hamiltonian matrix,

$$H_{\lambda k,\lambda' k'}^J = -\frac{\hbar^2}{2}\sum_{a,b}\bar{\mu}_{ab}^{\lambda\lambda'}\left\langle \phi_{km}^J \left| \frac{\partial^2}{\partial \xi_a \partial \xi_b} \right| \phi_{k'm'}^{*J} \right\rangle \delta_{JJ'}\delta_{mm'}, \quad \text{(A26)}$$

it can be seen that they differ significantly in magnitude, depending on whether they are diagonal in the vibrations, $\lambda = \lambda'$, or couple different vibrational states, $\lambda \neq \lambda'$. For semi-rigid molecules with small values of the vibrational quantum numbers, the following condition usually holds:

$$\left|H_{\lambda k,\lambda k'}^J\right| > \left|H_{\lambda k,\lambda' k'}^J\right|, \lambda \neq \lambda'. \quad \text{(A27)}$$

This results from the slight change in the effective geometry of the molecule upon vibrational excitation

$$|\mu_{ab}(0)| > \left| \sum_m \left(\frac{\partial \mu_{ab}(\underline{q})}{\partial q_m}\right)_0 \left\langle \Phi_\lambda^{\text{vib}} | q_m | \Phi_{\lambda'}^{\text{vib}} \right\rangle + \frac{1}{2}\sum_{m,n}\left(\frac{\partial^2 \mu_{ab}(\underline{q})}{\partial q_m \partial q_n}\right)_0 \left\langle \Phi_\lambda^{\text{vib}} | q_m q_n | \Phi_{\lambda'}^{\text{vib}} \right\rangle \right| \quad \text{(A28)}$$

and

$$\left|\bar{\mu}_{ab}^{\lambda\lambda}\right| > \left|\bar{\mu}_{ab}^{\lambda\lambda'}\right|, \quad \lambda \neq \lambda'. \quad \text{(A29)}$$

When calculating the vibrational–rotational energy levels, the off-diagonal elements $H_{\lambda k,\lambda' k'}^J$ corresponding to different vibrational states $\lambda \neq \lambda'$ give a much smaller contribution (change in the diagonal elements in the block that will be diagonalised) to the calculated energy levels than the non-diagonal elements $H_{\lambda k,\lambda k'}^J$ within the vibrational state in question. These changes are given approximately by

$$\Delta E_{\lambda\lambda'} = \frac{\left(H_{\lambda k,\lambda' k'}^J\right)^2}{H_{\lambda k,\lambda k}^J - H_{\lambda' k',\lambda' k'}^J}, \quad \text{(A30)}$$

$$\Delta E_{\lambda\lambda} = \frac{\left(H_{\lambda k,\lambda k'}^J\right)^2}{H_{\lambda k,\lambda k}^J - H_{\lambda k',\lambda k'}^J}. \quad \text{(A31)}$$

However,

$$\left|H_{\lambda k,\lambda k}^J - H_{\lambda' k',\lambda' k'}^J\right| \gg \left|H_{\lambda k,\lambda k}^J - H_{\lambda k',\lambda k'}^J\right|, \quad \text{(A32)}$$

since $(H_{\lambda k,\lambda k}^J - H_{\lambda k',\lambda k'}^J)$ involves only a change in the rotational energy level, while $(H_{\lambda k,\lambda k}^J - H_{\lambda' k',\lambda' k'}^J)$ involves also a change in the vibrational energy level.